Numer. Math. Theor. Meth. Appl.
doi: 10.4208/nmtma.OA-2023-0109

Vol. **xx**, No. x, pp. 1-36
x 2024

Novel Partitioned Time-Stepping Algorithms for Fast Computation of Random Interface-Coupled Problems with Uncertain Parameters

Yizhong Sun[1], Jiangshan Wang[1,*] and Haibiao Zheng[2]

[1] *School of Mathematical Sciences, East China Normal University, Shanghai, China*
[2] *School of Mathematical Sciences, Ministry of Education Key Laboratory of Mathematics and Engineering Applications, Shanghai Key Laboratory of PMMP, East China Normal University, Shanghai, China*

Received 15 September 2023; Accepted (in revised version) 5 October 2023

Abstract. The simulation of multi-domain, multi-physics mathematical models with uncertain parameters can be quite demanding in terms of algorithm design and computation costs. Our main objective in this paper is to examine a physical interface coupling between two random dissipative systems with uncertain parameters. Due to the complexity and uncertainty inherent in such interface-coupled problems, uncertain diffusion coefficients or friction parameters often arise, leading to considering random systems. We employ Monte Carlo methods to produce independent and identically distributed deterministic heat-heat model samples to address random systems, and adroitly integrate the ensemble idea to facilitate the fast calculation of these samples. To achieve unconditional stability, we introduce the scalar auxiliary variable (SAV) method to overcome the time constraints of the ensemble implicit-explicit algorithm. Furthermore, for a more accurate and stable scheme, the ensemble data-passing algorithm is raised, which is unconditionally stable and convergent without any auxiliary variables. These algorithms employ the same coefficient matrix for multiple linear systems and enable easy parallelization, which can significantly reduce the computational cost. Finally, numerical experiments are conducted to support the theoretical results and showcase the unique features of the proposed algorithms.

AMS subject classifications: 65M55, 65M60

Key words: Scalar auxiliary variable, ensemble algorithm, random interface-coupled problems, implicit-explicit partitioned method, data-passing partitioned method.

*Corresponding author. *Email addresses:* bill950204@126.com (Y. Sun), 52215500018@stu.ecnu.edu.cn (J. Wang), hbzheng@math.ecnu.edu.cn (H. Zheng)

1. Introduction

In the realm of mathematical physics, models of atmosphere-ocean interaction are commonly constructed by two incompressible Newtonian fluids along with compatible interface conditions [2, 20–22]. Recently, much focus has been placed on multi-domain, multi-physics coupled problems [1, 3, 8, 10, 16, 28], with particular interest in novel numerical simulations for fluid-fluid interaction models [5–7, 29]. In the study outlined by [6], a simplified atmosphere-ocean interaction model is considered, featuring a deterministic friction parameter κ and is deemed a linear heat-heat coupled system. To decouple such a multi-domain, multi-physics system naturally resulting in parallel computation, Connors *et al.* [6] presented the implicit-explicit (IMEX) and data-passing partitioned methods, which are both first-order in time, fully discrete methods. The most noteworthy aspect of [6] is illustrated by the fact that the data-passing partitioned method is unconditionally stable and convergent. Subsequently, in the case of the atmosphere-ocean interaction model incorporating some nonlinear interface demands, Connors *et al.* [7] built on existing research [6] and furthered an unconditionally stable method by executing geometric averaging for nonlinear terms.

Due to the inaccuracy of observation data, the complexity of the atmosphere-ocean coupling, or the introduction of additional uncertainty sources, the friction parameter κ [5] and diffusion coefficients ν_1, ν_2 [23] are physically impossible to determine, which can only give an approximate value range or meet a certain probability distribution. Therefore, exploring the numerical simulation of such problems with uncertain inputs is necessary. Uncertain parameters are often considered random functions determined by specific covariance structures, typically experimentally constructed basic random fields. In this paper, we focus on the linear heat-heat interface-coupled problems with three random coefficients κ, ν_1, and ν_2 as simplified fluid-fluid models. The main issue of this paper is to establish effective numerical schemes based on the ensemble idea, existing IMEX, and data-passing partitioned schemes, to achieve unconditional stability and fast computation for the random interface-coupled model.

One of the most popular approaches to address random problems is the Monte Carlo method [23, 24]. This involves transforming these random problems into a series of traditional PDEs that can be tackled by existing standard numerical methods. However, the solution's uncertainty and sensitivity require more samples for better estimation, which can lead to slow convergence rates. As a result, numerous linear equations with different stiffness matrices are formed, necessitating extensive computational costs. To increase efficiency and tackle these computational challenges, researchers proposed a fast ensemble time-stepping algorithm [12] to solve J (the number of samples) Navier-Stokes equations with different initial conditions and forcing terms. Jiang *et al.* [12] skillfully put forward the ensemble idea, at each time step, to solve the linear systems with a shared coefficient matrix and J right-hand sides. As only one efficient iterative solver was required for multiple linear systems with a common coefficient matrix, this significantly reduced storage requirements and computing costs. For uncertainties in initial conditions and forcing terms, the ensemble algorithm

has been extensively studied [12–15, 23–25]. Moreover, Wang *et al.* [23] first used this approach to solve parabolic problems with random parameters in space and time, making it an excellent reference for our theoretical analysis.

The scalar auxiliary variable method was initially proposed by [26,27] in the gradient flow problem. In recent years, the SAV method has gained popularity due to its ability to overcome the shortcomings of the invariant energy quantization (IEQ) approach while inheriting its benefits. This approach enables unconditional stability without the need for the energy density to be bound from below or solving linear equations with variable coefficients [4, 11, 18, 19, 27]. The SAV approach is widely used today for its advantages. He *et al.* [17] designed an SAV algorithm to obtain unconditional stability for fluid-fluid models with nonlinear interface conditions. Li *et al.* [18] constructed unconditional energy-stable pressure correction schemes for the Navier-Stokes equations by the SAV approach.

In the present work, we initially introduce the Monte Carlo algorithm for solving random interface-coupled problems and demonstrate that its convergence is influenced by both the Monte Carlo method and classical numerical methods. Subsequently, our primary focus is on proposing innovative numerical methods for the second step of the Monte Carlo algorithm. Drawing inspiration from [6], we develop an algorithm based on a standard partitioned time-stepping method known as the IMEX scheme. This algorithm can directly make the random friction parameters κ explicit, thereby reducing computation time. However, the stability of the IMEX scheme itself is affected by time constraints. To overcome this limitation, we combine it with the SAV method to achieve unconditional stability. Additionally, we address the randomness of the diffusion coefficients ν_1, ν_2 through an ensemble approach, leading us to create the SAV ensemble algorithm for the IMEX scheme. Furthermore, based on findings from [6], we discover that the data-passing scheme offers improved accuracy and stability compared to the IMEX scheme while maintaining unconditional stability and convergence. And the SAV method doubles the equations that need to be solved, which in turn increases the computational cost. Thus, we design an ensemble algorithm for the data-passing scheme, eliminating the need for auxiliary variables, although all three random parameters κ, ν_1, ν_2 require processing using the ensemble idea. In summary, we have obtained the following significant results:

- For the random interface-coupled problems: The proposed Monte Carlo algorithm has been shown to have a rigorous convergence rate (Theorem 2.1). This reflects the disadvantage of the Monte Carlo method, which typically has a slow convergence rate of $1/\sqrt{J}$. Moreover, the convergence result also shows the error estimate contributed by the finite element approximation.

- For IMEX scheme: We propose the SAV ensemble algorithm for the IMEX scheme (A1), which offers both unconditional stability and convergence. More importantly, the ensemble approach we introduce allows the use of the same coefficient matrix for multiple linear systems, which drastically reduces the computational cost.

- For data-passing scheme: The ensemble algorithm for the data-passing scheme (A2) is proposed while still maintaining unconditional stability and convergence without any auxiliary variables. Additionally, compared to the single domain problem presented in [23], we avoid imposing any stronger constraint conditions. It is worth noting that the random diffusion coefficients ν_1, ν_2 may change not only with space but also with time, causing the coefficient matrix to update with each time step. To further optimize the A2 algorithm and reduce calculation costs, we use a clever time-based averaging technique to estimate the coefficients ν_1, ν_2. There are no restrictions that need to be added or strengthened to ensure unconditional stability and convergence. The random friction parameter κ in both algorithms can simulate a range of real-world problems with large disturbances, typically between 10^{-3} and 10^3.

The paper is structured as follows. In Section 2, we introduce the random heat-heat coupled model along with relevant mathematical preliminaries, and we also discuss the Monte Carlo algorithm and its convergence. Section 3 presents the efficient SAV ensemble algorithm for the IMEX scheme, which we rigorously prove to have unconditional stability and convergence. In Section 4, we propose two ensemble algorithms based on the data-passing scheme, and show the stability and error estimation of both algorithms. Finally, Section 5 includes numerical tests that demonstrate the effectiveness of the proposed algorithms.

2. The random interface-coupled problems

In this paper, we will explore a pair of dissipative systems that are interconnected via interface conditions, enabling energy conversion at a single interface. Let the domain $\Omega \subset \mathbb{R}^d$ $(d = 2, 3)$ have convex, subdomains Ω_i $(i = 1, 2)$ with the interface $\Gamma = \partial\Omega_1 \cap \partial\Omega_2 = \bar{\Omega}_1 \cap \bar{\Omega}_2$ and outer boundary of each subdomain $\Gamma_i = \partial\Omega_i \backslash \Gamma$. The unit outward normal vectors on $\partial\Omega_1$ and $\partial\Omega_2$ are designated as $\hat{n}_1$ and $\hat{n}_2$, respectively. Fig. 1 is a simple 2D diagram to facilitate comprehension.

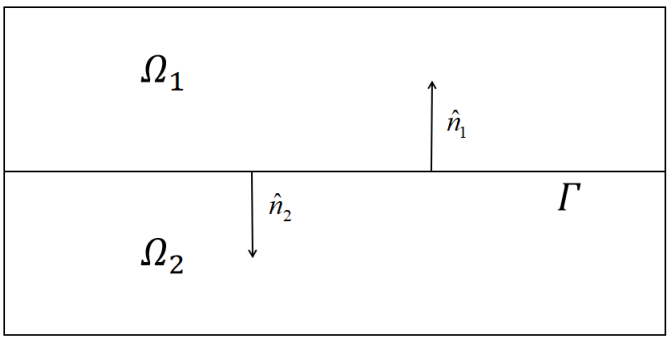

Figure 1: Example sub-domains, adjoined by an interface Γ.

The two heat equations coupled by the jump interface conditions are shown as follows:

$$u_{i,t} - \nabla \cdot \big(\nu_i(\mathbf{x},t)\nabla u_i\big) = f_i \quad \text{in } \Omega_i \times [0,T], \tag{2.1}$$

$$-\nu_i(\mathbf{x},t)\nabla u_i \cdot \hat{n}_i = \kappa(u_i - u_k) \quad \text{on } \Gamma \times [0,T], \quad i,k = 1,2, \quad i \neq k, \tag{2.2}$$

$$u_i(\mathbf{x},0) = u_i^0(\mathbf{x}) \quad \text{in } \Omega_i \times [0,T], \tag{2.3}$$

$$u_i(\mathbf{x},t) = 0 \quad \text{on } \Gamma_i = \partial\Omega_i \backslash \Gamma, \tag{2.4}$$

where $\nu_i \in L^2(W^{1,\infty}(\Omega);0,T)$ denotes the diffusion coefficient, $f_i \in L^2(H^{-1}(\Omega);0,T)$ is the sink/source term, and $\kappa > 0$ means the friction parameter, which is calculated in practice from bulk flux formulae [5].

We use $\|\cdot\|$ and $(\cdot,\cdot)$ to denote the L^2-norm and inner product on each subdomain, and $\|\cdot\|_\Gamma$ to denote the $L^2(\Gamma)$-norm on the interface. Let

$$X_i := \{v_i \in H^1(\Omega_i) : v_i = 0 \text{ on } \Gamma_i\}, \quad i = 1,2$$

be the Sobolev space for each subdomain. We define

$$X = X_1 \times X_2 = \big\{\mathbf{v} = (v_1, v_2) : v_i \in X_i,\ i = 1,2\big\},$$
$$L^2(\Omega) = L^2(\Omega_1) \times L^2(\Omega_2)$$

as two product spaces for the global domain. Moreover, the product spaces $L^2(\Omega)$ and X are equipped with the following norms:

$$\|\mathbf{v}\| = \sum_{i=1,2} \left(\int_{\Omega_i} |v_i|^2 dx \right)^{\frac{1}{2}},$$

$$\|\mathbf{v}\|_X = \sum_{i=1,2} \left(\int_{\Omega_i} \left(|v_i|^2 + |\nabla v_i|^2\right) dx \right)^{\frac{1}{2}}.$$

Consider a regular, quasi-uniform triangulation ($d = 2$) or tetrahedron ($d = 3$) $\mathcal{T}_i$ with mesh scale h for each subdomain Ω_i. We assume that $\mathcal{T}_1$ and $\mathcal{T}_2$ are compatible at the interface Γ and $\mathcal{T}_1 \cup \mathcal{T}_2 = \mathcal{T}_h$ is defined for the global domain Ω. Let $X_{i,h} \subset X_i$ be the finite element spaces for $i = 1,2$, which need to satisfy $X_h = X_{1,h} \times X_{2,h} \subset X$. The simulation time T can be divided into N smaller time intervals with $[0,T] = \cup_{n=0}^{N-1}[t^n, t^{n+1}]$, where $t^n = n\Delta t$, $\Delta t = T/N$.

Furthermore, we recall the Poincaré inequality and trace inequality as follows. There exist positive constants C_p and C_t only depending on the domain Ω such that

$$\|\mathbf{v}\| \leq C_p \|\nabla \mathbf{v}\|, \quad \|\mathbf{v}\|_\Gamma \leq C_t \|\mathbf{v}\|^{\frac{1}{2}} \|\nabla \mathbf{v}\|^{\frac{1}{2}}.$$

With the mesh-independent constant C, we assume the optimal approximation properties for piecewise continuous polynomials on the quasi-uniform mesh of local l as below

$$\inf_{v \in X_{i,h}} \|u - v\| \leq C h^{l+1} |u|_{H^{l+1}}, \quad \inf_{v \in X_{i,h}} \|u - v\|_{X_i} \leq C h^l |u|_{H^{l+1}}, \quad i = 1,2.$$

Due to the uncertainty in the observation data and the complexity of the atmosphere-ocean coupling, the diffusion coefficients ν_1, ν_2, and the friction parameter κ are physically difficult to determine. Furthermore, additional sources of uncertainty may be required to obtain κ [5]. This forces us to further investigate the random heat-heat interface-coupled model with three random coefficients κ, ν_1, and ν_2. Let $(\Pi, \mathcal{F}, \mathcal{P})$ be a complete probability space, where Π is the set of outcomes, $\mathcal{F} \subset 2^{\Pi}$ is the σ-algebra of events, and $\mathcal{P} : \mathcal{F} \to [0,1]$ is a probability measure. That is, the random heat-heat interface-coupled system reads: Find the random function u_i: $\Pi \times \Omega_i \times [0,T] \to \mathbb{R}$ satisfying $\mathcal{P}$ - a.e.

$$u_{i,t} - \nabla \cdot (\nu_i(\omega, \mathbf{x}, t)\nabla u_i) = f_i(\omega, \mathbf{x}, t) \quad \text{in } \Pi \times \Omega_i \times [0,T], \tag{2.5}$$

$$-\nu_i(\omega, \mathbf{x}, t)\nabla u_i \cdot \hat{n}_i = \kappa(\omega)(u_i - u_k) \quad \text{on } \Pi \times \Gamma \times [0,T], \quad i,k = 1,2, \quad i \neq k, \tag{2.6}$$

$$u_i(\omega, \mathbf{x}, 0) = u_i^0(\omega, \mathbf{x}) \quad \text{in } \Pi \times \Omega_i \times [0,T], \tag{2.7}$$

$$u_i(\omega, \mathbf{x}, t) = 0 \quad \text{on } \Pi \times \Gamma_i = \partial\Omega_i \backslash \Gamma, \tag{2.8}$$

where the diffusion coefficient ν_i and source force f_i hold: $\Pi \times \Omega_i \times [0,T] \to \mathbb{R}$, and $u_i^0 : \Pi \times \Omega_i \to \mathbb{R}$, which are assumed to have continuous and bounded covariance functions.

For the random system (2.5)-(2.8), we propose a Monte Carlo algorithm for the random interface-coupled problem, which consists of the following step:

1. Choose a set of independently, identically distributed (i.i.d) samples for the random friction parameter $\kappa(\omega_j)$ and diffusion coefficients $\nu_i(\omega_j, \cdot, \cdot)$, $j = 1, \ldots, J$.
2. Apply standard numerical methods to solve the corresponding deterministic PDEs for approximate solutions $u_{1,j}^{n+1}$ and $u_{2,j}^{n+1}$, $j = 1, \ldots, J$.
3. Approximate expectation $E[\mathbf{u}]$ by averaging the statistical information of the outputs $E[\mathbf{u}] \approx (\sum_{j=1}^{J} \mathbf{u}(\omega_j, \mathbf{x}, t))/J$.

Regarding random friction parameter $\kappa(\omega_j)$ as κ_j, and random diffusion coefficients $\nu_i(\omega_j, \mathbf{x}, t)$ as $\nu_{i,j}$, similarly denoting sink/source term $f_i(\omega_j, \mathbf{x}, t)$ as $f_{i,j}$, we have an ensemble of J heat-heat interface-coupled systems corresponding to J different parameters sets $(f_{i,j}, \kappa_j, \nu_{i,j})$, $i = 1,2$, $j = 1, \ldots, J$ as follows:

$$u_{i,j,t} - \nabla \cdot (\nu_{i,j}\nabla u_{i,j}) = f_{i,j} \quad \text{in } \Omega_i \times [0,T], \tag{2.9}$$

$$-\nu_{i,j}\nabla u_{i,j} \cdot \hat{n}_i = \kappa_j(u_{i,j} - u_{k,j}) \quad \text{on } \Gamma \times [0,T], \quad i,k = 1,2, \quad i \neq k, \tag{2.10}$$

$$u_{i,j}(\mathbf{x}, 0) = u_{i,j}^0(\mathbf{x}) \quad \text{in } \Omega_i \times [0,T], \tag{2.11}$$

$$u_{i,j}(\mathbf{x}, t) = 0 \quad \text{on } \Gamma_i = \partial\Omega_i \backslash \Gamma. \tag{2.12}$$

Then, the weak formulation of (2.9)-(2.12) can be written as follows: For $i,k = 1,2$, $i \neq k$ find $u_{i,j} : [0,T] \to X_i$ satisfying

$$(u_{i,j,t}, v_i) + (\nu_{i,j}\nabla u_{i,j}, \nabla v_i) + \int_{\Gamma} \kappa_j(u_{i,j} - u_{k,j})v_i \mathrm{d}s = (f_{i,j}, v_i), \quad \forall v_i \in X_i. \tag{2.13}$$

The natural monolithic weak formulation of the problem (2.9)-(2.12), found by summing (2.13) over $i = 1, 2$, is: Find $\mathbf{u}_j : [0, T] \to X$ satisfying

$$(\mathbf{u}_{j,t}, \mathbf{v}) + (\nu_j \nabla \mathbf{u}_j, \nabla \mathbf{v}) + \int_\Gamma \kappa_j [\mathbf{u}_j][\mathbf{v}] \mathrm{d}s = (\mathbf{f}_j, \mathbf{v}), \quad \forall \mathbf{v} \in X, \tag{2.14}$$

where $[\cdot]$ denotes the jump of the indicated quantity across the interface Γ and

$$(\mathbf{u}_{j,t}, \mathbf{v}) = \sum_{i=1}^{2} (u_{i,j,t}, v_i), \quad (\nu_j \nabla \mathbf{u}_j, \nabla \mathbf{v}) = \sum_{i=1}^{2} (\nu_{i,j} \nabla u_{i,j}, \nabla v_i), \quad (\mathbf{f}_j, \mathbf{v}) = \sum_{i=1}^{2} (f_{i,j}, v_i).$$

To obtain the convergence of the Monte Carlo algorithm, supposing

$$\tilde{\nu}_i = \frac{1}{J} \sum_{j=1}^{J} \nu_i(\omega_j, \mathbf{x}, t),$$

the following two conditions are valid:

(i) There exists a positive constant $\tilde{\theta}$, such that, for any $t \in [0, T]$,

$$P\left\{\omega \in \Omega;\ \min_{\mathbf{x} \in \bar{\Omega}} \tilde{\nu}_i(\omega, \mathbf{x}, t) \geq \tilde{\theta}\right\} = 1. \tag{2.15}$$

(ii) There exist positive constants $\tilde{\theta}_-$ and $\tilde{\theta}_+$, such that, for any $t \in [0, T]$,

$$P\left\{\omega_j \in \Omega;\ \tilde{\theta}_- \leq |\nu_i(\omega_j, \mathbf{x}, t) - \tilde{\nu}_i(\mathbf{x}, t)|_\infty \leq \tilde{\theta}_+\right\} = 1. \tag{2.16}$$

Theorem 2.1. *Under conditions (i)-(ii), assuming $\tilde{\theta} > \tilde{\theta}_+$ and $\Phi^n = (\sum_{j=1}^{J} \mathbf{u}_j^n)/J$, we have the following error estimation for the random interface-coupled system* (2.5)-(2.8)*:*

$$\begin{aligned}
&E\left[\|E[\mathbf{u}^{N+1}] - \Phi^{N+1}\|^2\right] + \kappa_{\max} \Delta t E\left[\|E[\mathbf{u}^{N+1}] - \Phi^{N+1}\|_\Gamma^2\right] \\
&\quad + \theta_- \Delta t E\left[\|\nabla E[\mathbf{u}^{N+1}] - \nabla \Phi^{N+1}\|^2\right] \\
&\quad + (\theta - \theta_+) \Delta t \sum_{n=0}^{N} E\left[\|\nabla E[\mathbf{u}^{n+1}] - \nabla \Phi^{n+1}\|^2\right] \\
&\leq \frac{1}{J}\left(E\left[\|\mathbf{u}_j^0\|^2\right] + C\Delta t E\left[\|\nabla \mathbf{u}_j^0\|^2\right] + C\Delta t E\left[\|\mathbf{u}_j^0\|_\Gamma^2\right] + C\Delta t \sum_{n=0}^{N} E\left[\|\mathbf{f}_j^{n+1}\|_{-1}^2\right]\right) \\
&\quad + C\big(\Delta t^2 + h^{2l}\big).
\end{aligned} \tag{2.17}$$

Proof. The error estimate result can be proved by analyzing two sources of error. The first source is the standard error of the Monte Carlo method, which follows the analysis in [23]. The second source is the error of the standard numerical methods,

inhere, the three novel partitioned time-stepping algorithms that will be constructed later. The proof of this part will also be given later (Theorems 3.2 and 4.2). □

When solving the corresponding deterministic PDEs with a standard numerical method, we need to solve the following linear systems:

$$A_{i,j}\left[\ u_i(\omega_j,\mathbf{x},t)\ \right]=\left[RHS_{i,j}(\mathbf{x})\right],\quad i=1,2,\quad j=1,\ldots,J.$$

More samples are required better to estimate the uncertainty and sensitivity of the solutions, which leads to a large number of linear equations with different stiffness matrices. To improve the computational efficiency, we hope to get an algebraic structure similar to that shown below

$$A_i\left[\ u_{i,1}\quad|\cdots|\quad u_{i,J}\ \right]=\left[RHS_{i,1}|\cdots|RHS_{i,J}\right],\quad i=1,2,$$

which shares the same coefficient matrix. Such an ensemble idea can make the coefficient matrices A_1 and A_2 only need to use once efficient iterative solves or direct solvers for fast computation. Hence, in this report, we mainly commit to presenting novel numerical algorithms for the second procedure of the Monte Carlo algorithm stated above. Drawing inspiration from [6], we will first develop an algorithm based on a standard partitioned time-stepping method known as the IMEX scheme in Section 3.

3. The SAV ensemble algorithm for IMEX scheme

In this section, we will establish an effective SAV ensemble algorithm based on the IMEX scheme for fast-solving the random heat-heat interface-coupled systems with three uncertain parameters. To overcome the time constraints inherent in the IMEX scheme itself, we first introduce a set of scalar auxiliary variables $q_j(t)=\exp(-t/T)$. Then, we can rewrite the weak formulation (2.13) as follows: for $i,k=1,2,\ i\neq k$, find $u_{i,j}:[0,T]\to X_i$ satisfying

$$\begin{aligned}&(u_{i,j,t},v_i)+(\nu_{i,j}\nabla u_{i,j},\nabla v_i)+\exp\left(\frac{t}{T}\right)q_j\int_\Gamma\kappa_j(u_{i,j}-u_{k,j})v_i\mathrm{d}s\\&=(f_{i,j},v_i),\quad\forall v_i\in X_i.\end{aligned}\tag{3.1}$$

Moreover, we can obtain the following equation:

$$\begin{aligned}\frac{dq_j}{dt}=&-\frac{1}{T}q_j+\exp\left(\frac{t}{T}\right)\sum_{i=1,i\neq k}^{2}\int_\Gamma\kappa_j(u_{i,j}-u_{k,j})u_{i,j}\mathrm{d}s\\&+\exp\left(\frac{2t}{T}\right)q_j\sum_{i=1,i\neq k}^{2}\int_\Gamma\kappa_j(u_{k,j}-u_{i,j})u_{i,j}\mathrm{d}s.\end{aligned}\tag{3.2}$$

Note that the last two interface terms in (3.2) add up to 0, but in the discrete case, they are not 0 and play a crucial role in subsequent analysis. The SAV ensemble algorithm for the IMEX scheme can be proposed as follows:

SAV ensemble algorithm for IMEX scheme (A1)

Let $\Delta t > 0$, $\bar{\nu}_i^n = (\sum_{j=1}^J \nu_{i,j}(\mathbf{x}, t^n))/J$, $\mathbf{u}_j^0 \in X_h$ and $\mathbf{f}_j \in L^2(H^{-1}(\Omega); 0, T))$ for $j = 1, \ldots, J$. Given $\mathbf{u}_j^n \in X_h$, for $n = 0, 1, 2, \ldots, N-1$ and $i, k = 1, 2$, $i \neq k$, we can find $\mathbf{u}_j^{n+1} \in X_h$ by

$$\left(\frac{u_{i,j}^{n+1} - u_{i,j}^n}{\Delta t}, v_i\right) + \left(\bar{\nu}_i^{n+1}\nabla u_{i,j}^{n+1}, \nabla v_i\right) + \left(\left(\nu_{i,j}^{n+1} - \bar{\nu}_i^{n+1}\right)\nabla u_{i,j}^n, \nabla v_i\right)$$
$$+ \exp\left(\frac{t^{n+1}}{T}\right) q_j^{n+1} \int_\Gamma \kappa_j \left(u_{i,j}^n - u_{k,j}^n\right) v_i \mathrm{d}s = \left(f_{i,j}^{n+1}, v_i\right), \quad \forall v_i \in X_{i,h}, \tag{3.3}$$

and

$$\begin{aligned}\frac{q_j^{n+1} - q_j^n}{\Delta t} = &-\frac{1}{T} q_j^{n+1} + \exp\left(\frac{t^{n+1}}{T}\right) \int_\Gamma \kappa_j \left(u_{1,j}^n - u_{2,j}^n\right) u_{1,j}^{n+1} \mathrm{d}s \\ &+ \exp\left(\frac{t^{n+1}}{T}\right) \int_\Gamma \kappa_j \left(u_{2,j}^n - u_{1,j}^n\right) u_{2,j}^{n+1} \mathrm{d}s \\ &+ \exp\left(\frac{2t^{n+1}}{T}\right) q_j^{n+1} \int_\Gamma \kappa_j \left(u_{2,j}^n - u_{1,j}^n\right) u_{1,j}^n \mathrm{d}s \\ &+ \exp\left(\frac{2t^{n+1}}{T}\right) q_j^{n+1} \int_\Gamma \kappa_j \left(u_{1,j}^n - u_{2,j}^n\right) u_{2,j}^n \mathrm{d}s. \end{aligned} \tag{3.4}$$

Such algorithm can directly decouple $u_{1,j}^{n+1}$ and $u_{2,j}^{n+1}$, but the scalar auxiliary variables q_j^{n+1} are still implicit. Therefore, this format can be used for theoretical analysis, and further processing of the algorithm is needed in numerical calculations. Let

$$S_j^{n+1} = \exp\left(\frac{t^{n+1}}{T}\right) q_j^{n+1}, \quad u_{i,j}^{n+1} = \hat{u}_{i,j}^{n+1} + S_j^{n+1} \check{u}_{i,j}^{n+1}, \quad i = 1, 2.$$

We can rewrite (3.3)-(3.4) as follows:

$$\left(\frac{\hat{u}_{i,j}^{n+1} - u_{i,j}^n}{\Delta t}, v_i\right) + \left(\bar{\nu}_i^{n+1}\nabla \hat{u}_{i,j}^{n+1}, \nabla v_i\right) + \left(\left(\nu_{i,j}^{n+1} - \bar{\nu}_i^{n+1}\right)\nabla u_{i,j}^n, \nabla v_i\right)$$
$$= \left(f_{i,j}^{n+1}, v_i\right), \quad \forall v_1 \in X_{i,h}, \tag{3.5}$$

$$\left(\frac{\check{u}_{i,j}^{n+1}}{\Delta t}, v_i\right) + \left(\bar{\nu}_i^{n+1}\nabla \check{u}_{i,j}^{n+1}, \nabla v_i\right) + \int_\Gamma \kappa_j \left(u_{i,j}^n - u_{i,j}^n\right) v_i \mathrm{d}s = 0, \quad \forall v_i \in X_{i,h}, \tag{3.6}$$

$$\left(\frac{T + \Delta t}{T\Delta t} - \exp\left(\frac{2t^{n+1}}{T}\right) A_1\right) S_j^{n+1} = \exp\left(\frac{t^{n+1}}{T}\right) \frac{q_j^n}{\Delta t} + \exp\left(\frac{2t^{n+1}}{T}\right) A_2, \tag{3.7}$$

where

$$A_1 = \int_\Gamma \kappa_j \left(u_{1,j}^n - u_{2,j}^n\right) \check{u}_{1,j}^{n+1} \mathrm{d}s + \int_\Gamma \kappa_j \left(u_{2,j}^n - u_{1,j}^n\right) \check{u}_{2,j}^{n+1} \mathrm{d}s$$

$$+\int_\Gamma \kappa_j(u_{2,j}^n-u_{1,j}^n)u_{1,j}^n\mathrm{d}s+\int_\Gamma \kappa_j\left(u_{1,j}^n-u_{2,j}^n\right)u_{2,j}^n\mathrm{d}s, \tag{3.8}$$

$$A_2=\int_\Gamma \kappa_j\left(u_{1,j}^n-u_{2,j}^n\right)\hat{u}_{1,j}^{n+1}\mathrm{d}s+\int_\Gamma \kappa_j\left(u_{2,j}^n-u_{1,j}^n\right)\hat{u}_{2,j}^{n+1}\mathrm{d}s. \tag{3.9}$$

Therefore, we can get $\hat{u}_{i,j}^{n+1}$, $\check{u}_{i,j}^{n+1}$ and S_j^{n+1} from (3.5)-(3.7), and final obtain $u_{i,j}^{n+1}$.

For the theoretical analysis, we suppose that the following two conditions are valid:

(iii) There exists a positive constant θ such that, for any $t\in[0,T]$,

$$\min_{\mathbf{x}\in\bar{\Omega}}\bar{\nu}_i(\mathbf{x},t)\geq\theta. \tag{3.10}$$

(iv) There exist positive constants θ_- and θ_+ such that, for any $t\in[0,T]$,

$$\theta_-\leq|\nu_{i,j}(\mathbf{x},t)-\bar{\nu}_i(\mathbf{x},t)|_\infty\leq\theta_+. \tag{3.11}$$

With the above assumptions, we can establish the stability of A1 as follows.

Theorem 3.1 (A1 Stability)**.** *Suppose that* $\mathbf{f}_j\in L^2(H^{-1}(\Omega);0,T)$ *and* $\mathbf{u}_j^{n+1}\in X_h$ *satisfy* (3.3) *for each* $n\in\{0,1,2,\ldots,N-1\}$*, and the conditions* (3.10)-(3.11) *holds, the algorithm A1 is stable on the premise that*

$$\theta>\theta_+. \tag{3.12}$$

Moreover, there exists a generic positive constant C *independent of* $h,\Delta t,J$ *such that*

$$\begin{aligned}&\left\|\mathbf{u}_j^N\right\|^2+\theta_+\Delta t\left\|\nabla\mathbf{u}_j^N\right\|^2+(\theta-\theta_+)\Delta t\sum_{n=0}^{N-1}\left\|\nabla\mathbf{u}_j^{n+1}\right\|^2+\left|q_j^N\right|^2\\&\quad+\frac{2\Delta t}{T}\sum_{n=0}^{N-1}\left|q_j^{n+1}\right|^2+2\Delta t\sum_{n=0}^{n-1}\exp\left(\frac{2t^{n+1}}{T}\right)\left|q_j^{n+1}\right|^2\int_\Gamma\kappa_j|u_{1,j}^n-u_{2,j}^n|^2\mathrm{d}s\\&\leq\left\|\mathbf{u}_j^0\right\|^2+C\Delta t\left\|\nabla\mathbf{u}_j^0\right\|^2+\left|q_j^0\right|^2+C\Delta t\sum_{n=0}^{n-1}\left\|\mathbf{f}_j^{n+1}\right\|_{-1}^2.\end{aligned} \tag{3.13}$$

Proof. Taking $\mathbf{v}=2\Delta t\mathbf{u}_j^{n+1}$ in (3.3), we have

$$\begin{aligned}&2\big(\mathbf{u}_j^{n+1}-\mathbf{u}_j^n,\mathbf{u}_j^{n+1}\big)+2\Delta t\big(\bar{\nu}^{n+1}\nabla\mathbf{u}_j^{n+1},\nabla\mathbf{u}_j^{n+1}\big)\\&\quad+2\exp\left(\frac{t^{n+1}}{T}\right)q_j^{n+1}\Delta t\int_\Gamma\kappa_j\big(u_{1,j}^n-u_{2,j}^n\big)u_{1,j}^{n+1}\mathrm{d}s\\&\quad+2\exp\left(\frac{t^{n+1}}{T}\right)q_j^{n+1}\Delta t\int_\Gamma\kappa_j\big(u_{2,j}^n-u_{1,j}^n\big)u_{2,j}^{n+1}\mathrm{d}s\\&\leq-2\Delta t\left(\big(\nu_j^{n+1}-\bar{\nu}^{n+1}\big)\nabla\mathbf{u}_j^n,\nabla\mathbf{u}_j^{n+1}\right)+2\Delta t\big(\mathbf{f}_j^{n+1},\mathbf{u}_j^{n+1}\big).\end{aligned} \tag{3.14}$$

Using the Young's inequality,

$$2(a-b,a) = a^2 + (a-b)^2 - b^2$$

and (3.10), we get

$$\begin{aligned}
&\|\mathbf{u}_j^{n+1}\|^2 - \|\mathbf{u}_j^n\|^2 + 2\theta\Delta t\|\nabla\mathbf{u}_j^{n+1}\|^2 \\
&\quad + 2\exp\left(\frac{t^{n+1}}{T}\right) q_j^{n+1}\Delta t\int_\Gamma \kappa_j\big(u_{1,j}^n - u_{2,j}^n\big)u_{1,j}^{n+1}\mathrm{d}s \\
&\quad + 2\exp\left(\frac{t^{n+1}}{T}\right) q_j^{n+1}\Delta t\int_\Gamma \kappa_j\big(u_{2,j}^n - u_{1,j}^n\big)u_{2,j}^{n+1}\mathrm{d}s \\
&\le -2\Delta t\left(\big(\nu_j^{n+1} - \bar\nu^{n+1}\big)\nabla\mathbf{u}_j^n, \nabla\mathbf{u}_j^{n+1}\right) + 2\Delta t\big(\mathbf{f}_j^{n+1}, \mathbf{u}_j^{n+1}\big).
\end{aligned} \tag{3.15}$$

Next, multiply the Eq. (3.4) by $2\Delta t q_j^{n+1}$ to address

$$\begin{aligned}
&\big|q_j^{n+1}\big|^2 - \big|q_j^n\big|^2 + \big|q_j^{n+1} - q_j^n\big|^2 + \frac{2\Delta t}{T}\big|q_j^{n+1}\big|^2 \\
&= 2\exp\left(\frac{t^{n+1}}{T}\right) q_j^{n+1}\Delta t\left(\int_\Gamma \kappa_j\big(u_{1,j}^n - u_{2,j}^n\big)u_{1,j}^{n+1}\mathrm{d}s + \int_\Gamma \kappa_j\big(u_{2,j}^n - u_{1,j}^n\big)u_{2,j}^{n+1}\mathrm{d}s\right) \\
&\quad + 2\exp\left(\frac{2t^{n+1}}{T}\right)\big|q_j^{n+1}\big|^2\Delta t\left(\int_\Gamma \kappa_j(u_{2,j}^n - u_{1,j}^n)u_{1,j}^n\mathrm{d}s + \int_\Gamma \kappa_j\big(u_{1,j}^n - u_{2,j}^n\big)u_{2,j}^n\mathrm{d}s\right).
\end{aligned} \tag{3.16}$$

Combining (3.15) and (3.16), we can obtain

$$\begin{aligned}
&\|\mathbf{u}_j^{n+1}\|^2 - \|\mathbf{u}_j^n\|^2 + 2\theta\Delta t\|\nabla\mathbf{u}_j^{n+1}\|^2 + \big|q_j^{n+1}\big|^2 - |q_j|^2 + \frac{2\Delta t}{T}\big|q_j^{n+1}\big|^2 \\
&\quad + 2\exp\left(\frac{2t^{n+1}}{T}\right)\big|q_j^{n+1}\big|^2\Delta t\int_\Gamma \kappa_j\big|u_{1,j}^n - u_{2,j}^n\big|^2\mathrm{d}s \\
&\le -2\Delta t\left(\big(\nu_j^{n+1} - \bar\nu^{n+1}\big)\nabla\mathbf{u}_j^n, \nabla\mathbf{u}_j^{n+1}\right) + 2\Delta t\big(\mathbf{f}_j^{n+1}, \mathbf{u}_j^{n+1}\big).
\end{aligned} \tag{3.17}$$

Applying the Cauchy-Schwarz and Young's inequalities on the right hand side (RHS), we have

$$2\Delta t\left(\big(\nu_j^{n+1} - \bar\nu^{n+1}\big)\nabla\mathbf{u}_j^n, \nabla\mathbf{u}_j^{n+1}\right) \le 2\theta_+\Delta t\left(\frac{\|\nabla\mathbf{u}_j^n\|^2}{2} + \frac{\|\nabla\mathbf{u}_j^{n+1}\|^2}{2}\right), \tag{3.18}$$

$$\big(\mathbf{f}_j^{n+1}, \mathbf{u}_j^{n+1}\big) \le \big\|\mathbf{f}_j^{n+1}\big\|_{-1}\big\|\nabla\mathbf{u}_j^{n+1}\big\| \le \frac{\Delta t}{2\alpha}\big\|\mathbf{f}_j^{n+1}\big\|_{-1}^2 + 2\alpha\Delta t\big\|\nabla\mathbf{u}_j^{n+1}\big\|^2. \tag{3.19}$$

Substitute (3.18)-(3.19) into (3.17) to yield the following result:

$$\begin{aligned}
&\|\mathbf{u}_j^{n+1}\|^2 - \|\mathbf{u}_j^n\|^2 + 2\Delta t\big(\theta - \theta_+ - \alpha\big)\|\nabla\mathbf{u}_j^{n+1}\|^2 \\
&\quad + \theta_+\Delta t\left(\big\|\nabla\mathbf{u}_j^{n+1}\big\|^2 - \big\|\nabla\mathbf{u}_j^n\big\|^2\right) + \big|q_j^{n+1}\big|^2 - \big|q_j^n\big|^2 + \frac{2\Delta t}{T}\big|q_j^{n+1}\big|^2 \\
&\quad + 2\exp\left(\frac{2t^{n+1}}{T}\right)\big|q_j^{n+1}\big|^2\Delta t\int_\Gamma \kappa_j\big|u_{1,j}^n - u_{2,j}^n\big|^2\mathrm{d}s \le \frac{\Delta t}{2\alpha}\big\|\mathbf{f}_j^{n+1}\big\|_{-1}^2.
\end{aligned} \tag{3.20}$$

Summing over $n = 0, 1, \ldots, N-1$, choosing $\alpha = (\theta - \theta_+)/2$, and using conditions (3.10), (3.12), we finally get

$$\begin{aligned}
&\left\|\mathbf{u}_j^N\right\|^2 + \theta_+\Delta t\left\|\nabla\mathbf{u}_j^N\right\|^2 + (\theta-\theta_+)\Delta t\sum_{n=0}^{N-1}\left\|\nabla\mathbf{u}_j^{n+1}\right\|^2 + \left|q_j^N\right|^2 \\
&\quad + \frac{2\Delta t}{T}\sum_{n=0}^{N-1}\left|q_j^{n+1}\right|^2 + 2\Delta t\sum_{n=0}^{n-1}\exp\left(\frac{2t^{n+1}}{T}\right)\left|q_j^{n+1}\right|^2\int_\Gamma \kappa_j|u_{1,j}^n - u_{2,j}^n|^2\mathrm{d}s \\
&\leq \left\|\mathbf{u}_j^0\right\|^2 + \theta_+\Delta t\left\|\nabla\mathbf{u}_j^0\right\|^2 + \left|q_j^0\right|^2 + \frac{\Delta t}{\theta-\theta_+}\sum_{n=0}^{n-1}\left\|\mathbf{f}_j^{n+1}\right\|_{-1}^2. \qquad (3.21)
\end{aligned}$$

The aforementioned is a comprehensive demonstration process. □

At this juncture, it is posited that C (with or without a subscript) denotes a generic positive constant regardless of the value of $h, \Delta t, J$. Moreover, it is worth noting that such constant may exhibit variability contingent upon the contextual circumstance. We can further estimate the approximation error of A1.

Theorem 3.2 (A1 Error Estimate). *Let $\mathbf{u}_j(t^{n+1})$ and $\mathbf{u}_j^{n+1}$ be the solutions of the natural monolithic weak formulation* (2.14) *and the algorithm A1 at time t^{n+1}, respectively. Assume $\mathbf{u}_t \in L^2(X;0,T), \mathbf{u}_{tt} \in L^2(L^2(\Omega);0,T)$, for all $t \in (0.T)$. If conditions* (3.10)-(3.11) *and the stability condition* (3.12) *hold, for any $n \in \{0,1,2,\ldots,N-1\}$, we can obtain the following error estimate for A1 with two generic positive constant C and C^* independent of $h, \Delta t, J$:*

$$\begin{aligned}
&\left\|\mathbf{u}_j(t^N) - \mathbf{u}_j^N\right\|^2 + \theta\Delta t\left\|\mathbf{u}_j(t^N) - \mathbf{u}_j^N\right\|^2 + \left|e_q^N\right|^2 + \frac{\Delta t}{T}\sum_{n=0}^{N-1}\left|e_q^{n+1}\right|^2 \\
&\leq C\exp\left(\Delta t\sum_{n=0}^{N-1}C^*\right)\Big\{\left\|\mathbf{u}_j(0) - \mathbf{u}_j^0\right\|^2 + \theta\Delta t\left\|\nabla(\mathbf{u}_j(0) - \mathbf{u}_j^0)\right\|^2 \\
&\qquad + \Delta t^2\|\mathbf{u}_{j,tt}\|_{L^2(0,T;L^2(\Omega))}^2 + \Delta t^2\|\nabla\mathbf{u}_{j,t}\|_{L^2(0,T;L^2(\Omega))}^2 \\
&\qquad + \inf_{\mathbf{v}_j^0\in X_h}\left\{\|\mathbf{u}_j(0) - \mathbf{v}_j^0\|^2 + \theta\Delta t\|\nabla(\mathbf{u}_j(0) - \mathbf{v}_j^0)\|^2\right\} \\
&\qquad + \inf_{\mathbf{v}_j\in X_h}\left\|(\mathbf{u}_j(t^n) - \mathbf{v}_j^n)_t\right\|_{L^2(0,T;L^2(\Omega))}^2 \\
&\qquad + T\max_{n=0,1,\ldots,N}\inf_{\mathbf{v}_j^n\in X_h}\left\|\nabla(\mathbf{u}_j(t^n) - \mathbf{v}_j^n)\right\|^2 + C\Delta t^2\Big\}. \qquad (3.22)
\end{aligned}$$

Proof. The proof of error estimates will be divided into the following three steps:

Step 1. We start by establishing an error equation corresponding to (3.3). Denoting the truncation error

$$\mathbf{r}_j^{n+1} = \mathbf{u}_{j,t}(t^{n+1}) - \frac{\mathbf{u}_j(t^{n+1}) - \mathbf{u}_j(t^n)}{\Delta t}$$

and subtracting (3.3) from (2.14), for any $\mathbf{v} \in \mathbf{X_h}$, we get the following error equation:

$$
\begin{aligned}
&(\mathbf{r}^{n+1}, \mathbf{v}) + \left(\frac{\mathbf{u}_j(t^{n+1}) - \mathbf{u}_j^{n+1}}{\Delta t} - \frac{\mathbf{u}_j(t^n) - \mathbf{u}_j^n}{\Delta t}, \mathbf{v} \right) \\
&\quad + \left(\bar{\nu}^{n+1} \big(\nabla \mathbf{u}_j(t^{n+1}) - \nabla \mathbf{u}_j^{n+1} \big), \nabla \mathbf{v} \right) \\
&\quad + \left(\big(\nu_j^{n+1} - \bar{\nu}^{n+1} \big) \big(\nabla \mathbf{u}_j(t^n) - \nabla \mathbf{u}_j^n \big), \nabla \mathbf{v} \right) \\
&\quad + \left(\big(\nu_j^{n+1} - \bar{\nu}^{n+1} \big) \big(\nabla \mathbf{u}_j(t^{n+1}) - \nabla \mathbf{u}_j(t^n) \big), \nabla \mathbf{v} \right) \\
&\quad + \exp\left(\frac{t^{n+1}}{T} \right) q_j(t^{n+1}) \sum_{i=1, i \neq k}^{2} \int_\Gamma \kappa_j \big[\mathbf{u}_j(t^{n+1}) \big] v_{i,j} \mathrm{d}s \\
&\quad - \exp\left(\frac{t^{n+1}}{T} \right) q_j^{n+1} \sum_{i=1, i \neq k}^{2} \int_\Gamma \kappa_j \big[\mathbf{u}_j^n \big] v_{i,j} \mathrm{d}s = 0.
\end{aligned} \tag{3.23}
$$

Some error functions are decomposed and defined as follows:

$$
\begin{aligned}
&\mathbf{u}_j(t^n) - \mathbf{u}_j^n = \big(\mathbf{u}_j(t^n) - \mathbf{v}_j^n \big) + \big(\mathbf{v}_j^n - \mathbf{u}_j^n \big) = \eta_j^n + \phi_j^n, \quad \forall \mathbf{v}_j^n \in X_h, \\
&e_q^{n+1} = q_j(t^{n+1}) - q_j^{n+1}.
\end{aligned}
$$

Choosing $\mathbf{v} = \phi_j^{n+1}$, we rewrite the error equation (3.23) as

$$
\begin{aligned}
&\frac{1}{2\Delta t} \left(\|\phi_j^{n+1}\|^2 - \|\phi_j^n\|^2 \right) + \theta \big\| \nabla \phi_j^{n+1} \big\|^2 \\
&\quad + \sum_{i=1, i \neq k}^{2} \int_\Gamma \kappa_j \big[\mathbf{u}_j(t^{n+1}) \big] \phi_{i,j}^{n+1} \mathrm{d}s \\
&\quad - \exp\left(\frac{t^{n+1}}{T} \right) q_j^{n+1} \sum_{i=1, i \neq k}^{2} \int_\Gamma \kappa_j \big[\mathbf{u}_j^n \big] \phi_{i,j}^{n+1} \mathrm{d}s \\
\leq\ & -\frac{1}{\Delta t} \left(\eta_j^{n+1} - \eta_j^n, \phi_{i,j}^{n+1} \right) - \left(\mathbf{r}_j^{n+1}, \phi_{i,j}^{n+1} \right) - \left(\bar{\nu}^{n+1} \nabla \eta_j^{n+1}, \nabla \phi_j^{n+1} \right) \\
&\quad - \left(\big(\nu_j^{n+1} - \bar{\nu}^{n+1} \big) \nabla \phi_j^n, \nabla \phi_j^{n+1} \right) - \left(\big(\nu_j^{n+1} - \bar{\nu}^{n+1} \big) \nabla \eta_j^n, \nabla \phi_j^{n+1} \right) \\
&\quad - \left(\big(\nu_j^{n+1} - \bar{\nu}^{n+1} \big) \big(\nabla \mathbf{u}_j(t^{n+1}) - \nabla \mathbf{u}_j(t^n) \big), \nabla \phi_j^{n+1} \right).
\end{aligned} \tag{3.24}
$$

Then, we can bound each term on the RHS of (3.24) with a series of positive constants $\xi_m,\ m = 1, 2, \ldots$. Applying Cauchy-Schwarz, Young's, and Poincaré inequalities for the RHS terms of (3.24), we can yield

$$
\left(\bar{\nu}^{n+1} \nabla \eta_j^{n+1}, \nabla \phi_j^{n+1} \right) \leq |\bar{\nu}^{n+1}|_\infty \left(\frac{\|\nabla \eta_j^{n+1}\|^2}{2\xi_1} + \frac{\xi_1 \|\nabla \phi_j^{n+1}\|^2}{2} \right), \tag{3.25}
$$

$$\Big(\big(\nu_j^{n+1}-\bar{\nu}^{n+1}\big)\nabla\phi_j^n,\nabla\phi_j^{n+1}\Big)\le\theta_+\left(\frac{\|\nabla\phi_j^n\|^2}{2\xi_2}+\frac{\xi_2\|\nabla\phi_j^{n+1}\|^2}{2}\right),\tag{3.26}$$

$$\Big(\big(\nu_j^{n+1}-\bar{\nu}^{n+1}\big)\nabla\eta_j^n,\nabla\phi_j^{n+1}\Big)\le\theta_+\left(\frac{\|\nabla\eta_j^n\|^2}{2\xi_3}+\frac{\xi_3\|\nabla\phi_j^{n+1}\|^2}{2}\right),\tag{3.27}$$

$$\begin{aligned}&\Big(\big(\nu_j^{n+1}-\bar{\nu}^{n+1}\big)\big(\nabla\mathbf{u}_j(t^{n+1})-\nabla\mathbf{u}_j(t^n)\big),\nabla\phi_j^{n+1}\Big)\\&\le\theta_+\left(\frac{\|\nabla(\mathbf{u}_j(t^{n+1})-\mathbf{u}_j(t^n))\|^2}{2\xi_4}+\frac{\xi_4\|\nabla\phi_j^{n+1}\|^2}{2}\right),\end{aligned}\tag{3.28}$$

$$\frac{1}{\Delta t}\Big(\eta_j^{n+1}-\eta_j^n,\phi_{i,j}^{n+1}\Big)\le\frac{C_p^2}{2\xi_5}\left\|\frac{\eta_j^{n+1}-\eta_j^n}{\Delta t}\right\|^2+\frac{\xi_5\|\nabla\phi_j^{n+1}\|^2}{2},\tag{3.29}$$

$$\Big(\mathbf{r}_j^{n+1},\phi_{i,j}^{n+1}\Big)\le\frac{C_p^2\|\mathbf{r}_j^{n+1}\|^2}{2\xi_6}+\frac{\xi_6\|\nabla\phi_j^{n+1}\|^2}{2}.\tag{3.30}$$

We can add and subtract the two terms

$$\sum_{i=1,i\neq k}^{2}\int_\Gamma\kappa_j\big[\mathbf{u}_j(t^n)\big]\phi_{i,j}^{n+1}\mathrm{d}s,\quad\sum_{i=1,i\neq k}^{2}\int_\Gamma\kappa_j\big[\mathbf{u}_j^n\big]\phi_{i,j}^{n+1}\mathrm{d}s$$

to treat the interface terms of (3.24)

$$\begin{aligned}&\sum_{i=1,i\neq k}^{2}\int_\Gamma\kappa_j\big[\mathbf{u}_j(t^{n+1})\big]\phi_{i,j}^{n+1}\mathrm{d}s-\exp\left(\frac{t^{n+1}}{T}\right)q_j^{n+1}\sum_{i=1,i\neq k}^{2}\int_\Gamma\kappa_j\big[\mathbf{u}_j^n\big]\phi_{i,j}^{n+1}\mathrm{d}s\\&=\left[\int_\Gamma\kappa_j\big(\mathbf{u}_j(t^{n+1})-\mathbf{u}_j(t^n)\big)\phi_j^{n+1}\mathrm{d}s-\int_\Gamma\kappa_j\big(u_{2,j}(t^{n+1})-u_{2,j}(t^n)\big)\phi_{1,j}^{n+1}\mathrm{d}s\right.\\&\qquad\left.-\int_\Gamma\kappa_j\big(u_{1,j}(t^{n+1})-u_{1,j}(t^n)\big)\phi_{2,j}^{n+1}\mathrm{d}s\right]\\&\quad+\left[\int_\Gamma\kappa_j\big(\mathbf{u}_j(t^n)-\mathbf{u}_j^n\big)\phi_j^{n+1}\mathrm{d}s-\int_\Gamma\kappa_j\big(u_{2,j}(t^n)-u_{2,j}^n\big)\phi_{1,j}^{n+1}\mathrm{d}s\right.\\&\qquad\left.-\int_\Gamma\kappa_j\big(u_{1,j}(t^n)-u_{1,j}^n\big)\phi_{2,j}^{n+1}\mathrm{d}s\right]\\&\quad+\left[\exp\left(\frac{t^{n+1}}{T}\right)e_q^{n+1}\int_\Gamma\kappa_j\big(u_{1,j}^n-u_{2,j}^n\big)\phi_{1,j}^{n+1}\mathrm{d}s\right.\\&\qquad\left.+\exp\left(\frac{t^{n+1}}{T}\right)e_q^{n+1}\int_\Gamma\kappa_j\big(u_{2,j}^n-u_{1,j}^n\big)\phi_{2,j}^{n+1}\mathrm{d}s\right]\\&=:B_1+B_2+B_3.\end{aligned}\tag{3.31}$$

Utilizing the trace theorem and Young's inequality for the RHS of (3.31), we get

$$\begin{aligned}
B_1 &\le C_t^2\kappa_j\|\nabla(\mathbf{u}_j(t^{n+1})-\mathbf{u}_j(t^n))\|\|\nabla\phi_j^{n+1}\| \\
&\quad + C_t^2\kappa_j\|\nabla(u_{2,j}(t^{n+1})-u_{2,j}(t^n)\|\|\nabla\phi_{1,j}^{n+1}\| \\
&\quad + C_t^2\kappa_j\|\nabla(u_{1,j}(t^{n+1})-u_{1,j}(t^n))\|\|\nabla\phi_{2,j}^{n+1}\| \\
&\le \frac{C\kappa_j^2}{\xi_7}\|\nabla(\mathbf{u}_j(t^{n+1})-\mathbf{u}_j(t^n))\|^2+\xi_7\|\nabla\phi_j^{n+1}\|^2, \qquad (3.32)
\end{aligned}$$

$$\begin{aligned}
B_2 &\le C\kappa_j\|\nabla\eta_j^n\|\|\nabla\phi_j^{n+1}\| + C\kappa_j\|\nabla\phi_j^n\|^{\frac12}\|\phi_j^n\|^{\frac12}\|\nabla\phi_j^{n+1}\|^{\frac12}\|\phi_j^{n+1}\|^{\frac12} \\
&\le \frac{C\kappa_j^2}{\xi_8}\|\nabla\eta_j^n\|^2+\xi_8\|\nabla\phi_j^{n+1}\|^2+\xi_9\|\nabla\phi_j^{n+1}\|^2 \\
&\quad + \frac{C\kappa_j^4}{\xi_9}\|\phi_j^{n+1}\|^2+\xi_{10}\|\nabla\phi_j^n\|^2+\frac{C}{\xi_{10}}\|\phi_j^n\|^2. \qquad (3.33)
\end{aligned}$$

Take

$$\begin{aligned}
&\xi_1=\frac{2\alpha\theta_+}{8|\bar\nu^{n+1}|_\infty}, && \xi_2=1, \\
&\xi_3=\xi_4=\frac{2\alpha}{8}, && \xi_5=\xi_6=\frac{2\alpha\theta_+}{8}, \\
&\xi_7=\xi_8=\xi_9=\frac{\alpha\theta_+}{8}, && \xi_{10}=\frac14(\theta-\theta_+),
\end{aligned}$$

where α is a positive constant and assuming $\theta>\theta_+$. Then, substitute the above inequalities (3.25)-(3.33) into (3.24) to obtain

$$\begin{aligned}
&\frac{1}{2\Delta t}\left(\|\phi_j^{n+1}\|^2-\|\phi_j^n\|^2\right)+\big(\theta-(1+\alpha)\theta_+\big)\|\nabla\phi_j^{n+1}\|^2 \\
&\quad+\frac{\theta_+}{2}\left(\|\nabla\phi_j^{n+1}\|^2-\|\nabla\phi_j^n\|^2\right)+B_3 \\
&\le \frac{C|\bar\nu^{n+1}|_\infty^2}{\alpha\theta_+}\|\nabla\eta_j^{n+1}\|^2+\frac{C\theta_+}{\alpha}\|\nabla\eta_j^n\|^2+\frac{C\kappa_j^2}{\alpha\theta_+}\|\nabla\eta_j^n\|^2 \\
&\quad+\frac{C\theta_+}{\alpha}\|\nabla(\mathbf{u}_j(t^{n+1})-\mathbf{u}_j(t^n))\|^2+\frac{C\kappa_j^2}{\alpha\theta_+}\|\nabla(\mathbf{u}_j(t^{n+1})-\mathbf{u}_j(t^n))\|^2 \\
&\quad+\frac{C}{\alpha\theta_+}\|\mathbf{r}_j^{n+1}\|^2+\frac{C}{\alpha\theta_+}\left\|\frac{\eta_j^{n+1}-\eta_j^n}{\Delta t}\right\|^2+\frac{C\kappa_j^4}{\alpha\theta_+}\|\phi_j^{n+1}\|^2 \\
&\quad+\frac{\theta-\theta_+}{4}\|\nabla\phi_j^n\|^2+\frac{C}{\theta-\theta_+}\|\phi_j^n\|^2. \qquad (3.34)
\end{aligned}$$

Setting $\alpha=(\theta-\theta_+)/2\theta_+$, we have

$$\theta-(1+\alpha)\theta_+>\frac{\theta-\theta_+}{2}>0$$

based on the stability condition (3.12) and the upper bound in condition (3.11). Then multiplying (3.34) by $2\Delta t$ and summing over $n=0,\dots,N-1$, we have

$$
\begin{aligned}
&\left\|\phi_j^N\right\|^2+(\theta-\theta_+)\Delta t\sum_{n=0}^{N-1}\left\|\nabla\phi_j^{n+1}\right\|^2-\frac{\theta-\theta_+}{2}\Delta t\sum_{n=0}^{N-1}\left\|\nabla\phi_j^n\right\|^2\\
&\quad+\theta_+\Delta t\left\|\nabla\phi_j^N\right\|^2+2\Delta t\sum_{n=0}^{N-1}B_3\\
&\le\Delta t\sum_{n=0}^{N-1}\left\{\frac{C|\bar\nu^{n+1}|_\infty^2}{\theta-\theta_+}\left\|\nabla\eta_j^{n+1}\right\|^2+\frac{C}{\theta-\theta_+}\left\|\nabla\eta_j^n\right\|^2\right.\\
&\qquad+\frac{C\kappa_j^2}{\theta-\theta_+}\left\|\nabla\eta_j^n\right\|^2+\frac{C}{\theta-\theta_+}\left\|\nabla(\mathbf{u}_j(t^{n+1})-\mathbf{u}_j(t^n))\right\|^2\\
&\qquad+\frac{C\kappa_j^2}{\theta-\theta_+}\left\|\nabla(\mathbf{u}_j(t^{n+1})-\mathbf{u}_j(t^n))\right\|^2+\frac{C}{\theta-\theta_+}\left\|\mathbf{r}_j^{n+1}\right\|^2\\
&\qquad\left.+\frac{C}{\theta-\theta_+}\left\|\frac{\eta_j^{n+1}-\eta_j^n}{\Delta t}\right\|^2+\frac{C\kappa_j^4}{\theta-\theta_+}\left\|\phi_j^{n+1}\right\|^2+\frac{C}{\theta-\theta_+}\left\|\phi_j^n\right\|^2\right\}\\
&\quad+\left\|\phi_j^0\right\|^2+\theta_+\Delta t\left\|\nabla\phi_j^0\right\|^2.
\end{aligned}
\tag{3.35}
$$

Step 2. We note that B_3 of (3.33) can not be easily bounded. We shall balance such term with a term from the error equation for q_j^{n+1}. Subtracting (3.4) from (3.1) leads to

$$
\begin{aligned}
&\frac{e_q^{n+1}-e_q^n}{\Delta t}+\frac{1}{T}e_q^{n+1}\\
&=\exp\left(\frac{t^{n+1}}{T}\right)\sum_{i=1,i\neq k}^{2}\left(\int_\Gamma\kappa_j\left[\mathbf{u}_j(t^{n+1})\right]u_{i,j}(t^{n+1})\mathrm{d}s-\int_\Gamma\kappa_j\left[\mathbf{u}_j^n\right]u_{i,j}^{n+1}\mathrm{d}s\right)\\
&\quad+\exp\left(\frac{2t^{n+1}}{T}\right)\sum_{i=1,i\neq k}^{2}\left(q_j^{n+1}\int_\Gamma\kappa_j\left[\mathbf{u}_j^n\right]u_{i,j}^n\mathrm{d}s-q_j(t^{n+1})\right.\\
&\qquad\left.\times\int_\Gamma\kappa_j\left[\mathbf{u}_j(t^{n+1})\right]u_{i,j}(t^{n+1})\mathrm{d}s\right)+r_q^{n+1},
\end{aligned}
\tag{3.36}
$$

where

$$
r_q^{n+1}=\frac{q_j(t^{n+1})-q_j(t^n)}{\Delta t}-q_{j,t}(t^{n+1})=\frac{1}{\Delta t}\int_{t^n}^{t^{n+1}}(t-t^n)q_{j,tt}\mathrm{d}t.
\tag{3.37}
$$

Multiply both sides of (3.36) by $2\Delta t e_q^{n+1}$ to yield

$$
\begin{aligned}
&\left|e_q^{n+1}\right|^2-\left|e_q^n\right|^2+\frac{2\Delta t}{T}\left|e_q^{n+1}\right|^2\\
&\le2\exp\left(\frac{t^{n+1}}{T}\right)e_q^{n+1}\Delta t\sum_{i=1,i\neq k}^{2}\left(\int_\Gamma\kappa_j\left[\mathbf{u}_j(t^{n+1})\right]u_{i,j}(t^{n+1})\mathrm{d}s-\int_\Gamma\kappa_j\left[\mathbf{u}_j^n\right]u_{i,j}^{n+1}\mathrm{d}s\right)
\end{aligned}
$$

$$+ 2\exp\left(\frac{2t^{n+1}}{T}\right) e_q^{n+1}\Delta t \sum_{i=1,i\neq k}^{2}\left(q_j^{n+1}\int_\Gamma \kappa_j\left[\mathbf{u}_j^n\right] u_{i,j}^n \mathrm{d}s - q_j(t^{n+1}) \times \int_\Gamma \kappa_j\left[\mathbf{u}_j(t^{n+1})\right] u_{i,j}(t^{n+1})\mathrm{d}s\right) + 2\Delta t r_q^{n+1} e_q^{n+1}. \quad (3.38)$$

Note that the first terms on the RHS of (3.38) holds

$$\begin{aligned}
&2\exp\left(\frac{t^{n+1}}{T}\right) e_q^{n+1}\Delta t \sum_{i=1,i\neq k}^{2}\left(\int_\Gamma \kappa_j[\mathbf{u}_j(t^{n+1})]u_{i,j}(t^{n+1})\mathrm{d}s - \int_\Gamma \kappa_j[\mathbf{u}_j^n]u_{i,j}^{n+1}\mathrm{d}s\right)\\
&= \left[2\exp\left(\frac{t^{n+1}}{T}\right) e_q^{n+1}\Delta t\Big(\int_\Gamma \kappa_j(\mathbf{u}_j(t^{n+1}) - \mathbf{u}_j(t^n))\mathbf{u}_j(t^{n+1})\mathrm{d}s \right.\\
&\qquad - \int_\Gamma \kappa_j(u_{2,j}(t^{n+1}) - u_{2,j}(t^n))u_{1,j}(t^{n+1})\mathrm{d}s\\
&\qquad \left. - \int_\Gamma \kappa_j(u_{1,j}(t^{n+1}) - u_{1,j}(t^n))u_{2,j}(t^{n+1})\mathrm{d}s\Big)\right]\\
&\quad + \left[2\exp\left(\frac{t^{n+1}}{T}\right) e_q^{n+1}\Delta t\Big(\int_\Gamma \kappa_j(\mathbf{u}_j(t^n) - \mathbf{u}_j^n)\mathbf{u}_j(t^{n+1})\mathrm{d}s \right.\\
&\qquad - \int_\Gamma \kappa_j(u_{2,j}(t^n) - u_{2,j}^n)u_{1,j}(t^{n+1})\mathrm{d}s\\
&\qquad \left. - \int_\Gamma \kappa_j(u_{1,j}(t^n) - u_{1,j}^n)u_{2,j}(t^{n+1})\mathrm{d}s\Big)\right]\\
&\quad + \left[2\exp\left(\frac{t^{n+1}}{T}\right) e_q^{n+1}\Delta t\Big(\int_\Gamma \kappa_j(u_{1,j}^n - u_{2,j}^n)\eta_{1,j}^{n+1}\mathrm{d}s \right.\\
&\qquad \left. + \int_\Gamma \kappa_j(u_{2,j}^n - u_{1,j}^n)\eta_{2,j}^{n+1}\mathrm{d}s\Big)\right]\\
&\quad + \left[2\exp\left(\frac{t^{n+1}}{T}\right) e_q^{n+1}\Delta t\Big(\int_\Gamma \kappa_j(u_{1,j}^n - u_{2,j}^n)\phi_{1,j}^{n+1}\mathrm{d}s \right.\\
&\qquad \left. + \int_\Gamma \kappa_j(u_{2,j}^n - u_{1,j}^n)\phi_{2,j}^{n+1}\mathrm{d}s\Big)\right]\\
&=: D_1 + D_2 + D_3 + D_4. \quad (3.39)
\end{aligned}$$

From the stability result (3.13), we have

$$\left\|u_{i,j}^{n+1}\right\| \le c_0, \quad \left|q_j^{n+1}\right| \le c_1, \quad \left|e_q^{n+1}\right| = \left|q_j(t^{n+1}) - q_j^{n+1}\right| \le \exp(1) + \left|q_j^{n+1}\right| \le c_2.$$

We can further estimate D_1, D_2, D_3 of (3.39) by Hölder and Young inequalities as follows:

$$D_1 \le 4\exp(1)\Delta t\kappa_j C_t^2 \left\|\nabla(\mathbf{u}_j(t^{n+1}) - \mathbf{u}_j(t^n))\right\| \left\|\nabla\mathbf{u}_j(t^{n+1})\right\| \left|e_q^{n+1}\right|$$

$$\leq C\kappa_j^2\Delta t\big\|\nabla(\mathbf{u}_j(t^{n+1})-\mathbf{u}_j(t^n))\big\|^2+\frac{\Delta t}{11T}\big|e_q^{n+1}\big|^2, \tag{3.40}$$

$$\begin{aligned}D_2&\leq 4\exp(1)\kappa_j\Delta t\big|e_q^{n+1}\big|\left(\big\|\nabla\eta_j^n\big\|+\big\|\phi_j^n\big\|^{\frac{1}{2}}\big\|\nabla\phi_j^n\big\|^{\frac{1}{2}}\right)\big\|\nabla\mathbf{u}_j(t^{n+1})\big\|\\&\leq\frac{2\Delta t}{11T}\big|e_q^{n+1}\big|^2+C\kappa_j^2\Delta t\big\|\nabla\eta_j^n\big\|^2+\xi_{11}\Delta t\big\|\nabla\phi_j^n\big\|^2+\frac{C\kappa_j^4\Delta t}{\xi_{11}}\big\|\phi_j^n\big\|^2,\end{aligned} \tag{3.41}$$

$$\begin{aligned}D_3&\leq 2\exp(1)\Delta t\kappa_jC_t^2\big|e_q^{n+1}\big|\left(\big\|\nabla(u_{1,j}^n-u_{2,j}^n)\big\|\big\|\nabla\eta_{1,j}^{n+1}\big\|+\big\|\nabla(u_{2,j}^n-u_{1,j}^n)\big\|\big\|\nabla\eta_{2,j}^{n+1}\big\|\right)\\&\leq C\kappa_j\Delta t\big|e_q^{n+1}\big|\big\|\nabla\eta_j^{n+1}\big\|\Big(\big\|\nabla\phi_j^n\big\|+\big\|\nabla\mathbf{v}_j^n\big\|\Big)\\&\leq\xi_{12}\Delta t\big\|\nabla\phi_j^n\big\|^2+\frac{C\kappa_j^2\Delta t}{\xi_{12}}\big\|\nabla\eta_j^{n+1}\big\|^2+\frac{\Delta t}{11T}\big|e_q^{n+1}\big|^2+C\kappa_j^2\Delta t\big\|\nabla\eta_j^{n+1}\big\|^2.\end{aligned} \tag{3.42}$$

The second term on the RHS of (3.38) can be written as

$$\begin{aligned}&2\exp\left(\frac{2t^{n+1}}{T}\right)e_q^{n+1}\Delta t\sum_{i=1,i\neq k}^{2}\left(q_j^{n+1}\int_\Gamma\kappa_j\left[\mathbf{u}_j^n\right]u_{i,j}^n\mathrm{d}s-q_j(t^{n+1})\right.\\&\qquad\left.\times\int_\Gamma\kappa_j\left[\mathbf{u}_j(t^{n+1})\right]u_{i,j}(t^{n+1})\mathrm{d}s\right)\\&=\left[2\exp\left(\frac{2t^{n+1}}{T}\right)e_q^{n+1}q_j^{n+1}\Delta t\sum_{i=1,i\neq k}^{2}\int_\Gamma\kappa_j\left[\mathbf{u}_j^n\right]\left(u_{i,j}^n-u_{i,j}(t^{n+1})\right)\mathrm{d}s\right]\\&\quad+\left[2\exp\left(\frac{2t^{n+1}}{T}\right)e_q^{n+1}q_j^{n+1}\Delta t\int_\Gamma\kappa_j\left(\left[\mathbf{u}_j^n\right]-\left[\mathbf{u}_j(t^{n+1})\right]\right)u_{i,j}(t^{n+1})\mathrm{d}s\right]\\&\quad-\left[2\exp\left(\frac{2t^{n+1}}{T}\right)\big|e_q^{n+1}\big|^2\Delta t\sum_{i=1,i\neq k}^{2}\left(\int_\Gamma\kappa_j\left[\mathbf{u}_j(t^{n+1})\right]u_{i,j}(t^{n+1})\mathrm{d}s\right)\right]\\&=:F_1+F_2-F_3.\end{aligned} \tag{3.43}$$

Then, applying the Hölder inequality and Young inequality, we can get

$$\begin{aligned}F_1&=2\exp\left(\frac{2t^{n+1}}{T}\right)e_q^{n+1}q_j^{n+1}\\&\quad\times\Delta t\Bigg(\int_\Gamma\kappa_j\big(u_{1,j}^n-u_{2,j}^n\big)\big(u_{1,j}^n-u_{1,j}(t^n)+u_{1,j}(t^n)-u_{1,j}(t^{n+1})\big)\\&\qquad+\int_\Gamma\kappa_j\big(u_{2,j}^n-u_{1,j}^n\big)\big(u_{2,j}^n-u_{2,j}(t^n)+u_{2,j}(t^n)-u_{2,j}(t^{n+1})\big)\Bigg)\\&\leq C\kappa_j\Delta t\big|e_q^{n+1}\big|\big|q_j^{n+1}\big|\big\|\nabla\mathbf{u}_j^n\big\|\left(\big\|\nabla\eta_j^n\big\|+\big\|\phi_j^n\big\|^{\frac{1}{2}}\big\|\nabla\phi_j^n\big\|^{\frac{1}{2}}+\big\|\nabla(\mathbf{u}_j(t^{n+1})-\mathbf{u}_j(t^n))\big\|\right)\\&\leq\xi_{13}\Delta t\big\|\nabla\phi_j^n\big\|^2+\frac{C\kappa_j^2\Delta t}{\xi_{13}}\big\|\nabla\eta_j^n\big\|^2+\xi_{14}\Delta t\big\|\nabla\phi_j^n\big\|^2+\frac{C\kappa_j^2\Delta t}{\xi_{14}}\big\|\phi_j^n\big\|^2+\xi_{15}\Delta t\big\|\nabla\phi_j^n\big\|^2\end{aligned}$$

$$+\frac{C\kappa_j^2\Delta t}{\xi_{15}}\left\|\nabla(\mathbf{u}_j(t^{n+1})-\mathbf{u}_j(t^n))\right\|^2+\frac{3\Delta t}{11T}\left|e_q^{n+1}\right|^2$$
$$+C\kappa_j^2\Delta t\left\|\nabla\eta_j^n\right\|^2+\xi_{16}\Delta t\left\|\nabla\phi_j^n\right\|^2$$
$$+\frac{C\kappa_j^4\Delta t}{\xi_{16}}\left\|\phi_j^n\right\|^2+C\kappa_j^2\Delta t\left\|\nabla(\mathbf{u}_j(t^{n+1})-\mathbf{u}_j(t^n))\right\|^2, \tag{3.44}$$

$$F_2\le\frac{3\Delta t}{11T}\left|e_q^{n+1}\right|^2+C\kappa_j^2\Delta t\left\|\nabla\eta_j^n\right\|^2+\xi_{17}\Delta t\left\|\nabla\phi_j^n\right\|^2+\frac{C\kappa_j^4\Delta t}{\xi_{17}}\left\|\phi_j^n\right\|^2$$
$$+C\kappa_j^2\Delta t\left\|\nabla(\mathbf{u}_j(t^{n+1})-\mathbf{u}_j(t^n))\right\|^2. \tag{3.45}$$

For the last term on the RHS of (3.38), we have

$$2\Delta t r_q^{n+1}e_q^{n+1}\le\frac{\Delta t}{11T}\left|e_q^{n+1}\right|^2+C\Delta t^2\int_{t^n}^{t^{n+1}}\left|q_{j,tt}\right|^2\mathrm{d}t. \tag{3.46}$$

Setting

$$\xi_{11}=\xi_{12}=\xi_{13}=\xi_{14}=\xi_{15}=\xi_{16}=\xi_{17}=\frac{1}{14}(\theta-\theta_+)$$

and combining (3.38) with (3.39)-(3.46) result in

$$\left|e_q^{n+1}\right|^2-\left|e_q^n\right|^2+\frac{\Delta t}{T}\left|e_q^{n+1}\right|^2-\frac{1}{2}\left(\theta-\theta_+\right)\Delta t\left\|\nabla\phi_j^n\right\|^2$$
$$\le C\kappa_j^2\Delta t\left\|\nabla(\mathbf{u}_j(t^{n+1})-\mathbf{u}_j(t^n))\right\|^2+C\kappa_j^2\Delta t\left\|\nabla\eta_j^n\right\|^2+C\kappa_j^2\Delta t\left\|\nabla\eta_j^{n+1}\right\|^2$$
$$+\frac{C\kappa_j^4\Delta t}{\theta-\theta_+}\left\|\phi_j^n\right\|^2+\frac{C\kappa_j^2\Delta t}{\theta-\theta_+}\left\|\phi_j^n\right\|^2+C\Delta t^2\int_{t^n}^{t^{n+1}}|q_{j,tt}|^2\mathrm{d}t+D_4+F_3. \tag{3.47}$$

By summing (3.47) from $n=0,\ldots,N-1$, we can arrive at

$$\left|e_q^N\right|^2+\frac{\Delta t}{T}\sum_{n=0}^{N-1}\left|e_q^{n+1}\right|^2-\frac{1}{2}\left(\theta-\theta_+\right)\Delta t\sum_{n=0}^{N-1}\left\|\nabla\phi_j^n\right\|^2$$
$$\le\sum_{n=0}^{N-1}\Big\{C\kappa_j^2\Delta t\left\|\nabla(\mathbf{u}_j(t^{n+1})-\mathbf{u}_j(t^n))\right\|^2$$
$$+C\kappa_j^2\Delta t\left\|\nabla\eta_j^n\right\|^2+C\kappa_j^2\Delta t\left\|\nabla\eta_j^{n+1}\right\|^2$$
$$+\frac{C\kappa_j^4\Delta t}{\theta-\theta_+}\left\|\phi_j^n\right\|^2+\frac{C\kappa_j^2\Delta t}{\theta-\theta_+}\left\|\phi_j^n\right\|^2$$
$$+C\Delta t^2\int_{t^n}^{t^{n+1}}|q_{j,tt}|^2\mathrm{d}t+D_4+F_3\Big\}. \tag{3.48}$$

Step 3. Combining (3.35) with (3.48) we have

$$\left\|\phi_j^N\right\|^2+\theta\Delta t\left\|\nabla\phi_j^N\right\|^2+\sum_{n=0}^{N-1}F_3+\left|e_q^N\right|^2+\frac{\Delta t}{T}\sum_{n=0}^{N-1}\left|e_q^{n+1}\right|^2\le\left\|\phi_j^0\right\|^2+\theta\Delta t\left\|\nabla\phi_j^0\right\|^2$$

$$
\begin{aligned}
&+\sum_{n=0}^{N-1}\Bigg\{C\left(\frac{|\bar{\nu}^{n+1}|_\infty^2}{\theta-\theta_+}+\kappa_j^2\right)\Delta t\big\|\nabla\eta_j^{n+1}\big\|^2\\
&\qquad+C\left(\frac{1}{\theta-\theta_+}+\frac{\kappa_j^2}{\theta-\theta_+}+\kappa_j^2\right)\Delta t\big\|\nabla\eta_j^{n}\big\|^2\\
&\qquad+C\left(\frac{1}{\theta-\theta_+}+\frac{\kappa_j^2}{\theta-\theta_+}+\kappa_j^2\right)\Delta t\big\|\nabla(\mathbf{u}_j(t^{n+1})-\mathbf{u}_j(t^n))\big\|^2\\
&\qquad+\frac{C\Delta t}{\theta-\theta_+}\big\|\mathbf{r}_j^{n+1}\big\|^2+\frac{C\Delta t}{\theta-\theta_+}\left\|\frac{\eta_j^{n+1}-\eta_j^n}{\Delta t}\right\|^2\\
&\qquad+C\Delta t^2\int_{t^n}^{t^{n+1}}|q_{j,tt}|^2\mathrm{d}t+\frac{C\kappa_j^4\Delta t}{\theta-\theta_+}\big\|\phi_j^{n+1}\big\|^2\\
&\qquad+C\left(\frac{1}{\theta-\theta_+}+\frac{\kappa_j^2}{\theta-\theta_+}+\frac{\kappa_j^4}{\theta-\theta_+}\right)\Delta t\big\|\phi_j^{n}\big\|^2\Bigg\}.
\end{aligned}\tag{3.49}
$$

Note that

$$
\begin{aligned}
F_3&=2\exp\left(\frac{2t^{n+1}}{T}\right)\left|e_q^{n+1}\right|^2\Delta t\sum_{i=1,i\neq k}^{2}\int_\Gamma\kappa_j\left[\mathbf{u}_j(t^{n+1})\right]u_{i,j}(t^{n+1})\mathrm{d}s\\
&=2\exp\left(\frac{2t^{n+1}}{T}\right)\left|e_q^{n+1}\right|^2\Delta t\int_\Gamma\kappa_j[\mathbf{u}_j(t^{n+1})]^2\mathrm{d}s\geq 0,
\end{aligned}\tag{3.50}
$$

and

$$
\Delta t\sum_{n=0}^{N-1}\left\|\frac{\eta_j^{n+1}-\eta_j^n}{\Delta t}\right\|^2\leq\int_0^{t^{n+1}}\|\eta_{j,t}\|^2\mathrm{d}t\leq\|\eta_{j,t}\|^2_{L^2(0,T;L^2(\Omega))},\tag{3.51}
$$

$$
\begin{aligned}
&\Delta t\sum_{n=0}^{N-1}\big\|\nabla(\mathbf{u}_j(t^{n+1})-\mathbf{u}_j(t^n))\big\|^2\leq\Delta t^2\int_0^{t^{n+1}}\|\nabla\mathbf{u}_{j,t}\|^2\mathrm{d}t\\
&\leq\Delta t^2\|\nabla\mathbf{u}_{j,t}\|^2_{L^2(0,T;L^2(\Omega))},
\end{aligned}\tag{3.52}
$$

$$
\Delta t\sum_{n=0}^{N-1}\big\|\mathbf{r}_j^{n+1}\big\|^2\leq\Delta t^2\int_0^{t^{n+1}}\|\mathbf{u}_{j,tt}\|^2\mathrm{d}t\leq\Delta t^2\|\mathbf{u}_{j,tt}\|^2_{L^2(0,T;L^2(\Omega))}.\tag{3.53}
$$

Taking infimum over $\mathbf{v}_j^n\in X_h$, using the triangle inequality to $\|\phi_j^0\|^2+\theta\Delta t\|\nabla\phi_j^0\|^2$, and combining with the inequalities (3.50)-(3.53), we can yield

$$
\begin{aligned}
&\big\|\phi_j^N\big\|^2+\theta\Delta t\big\|\nabla\phi_j^N\big\|^2+\left|e_q^N\right|^2+\frac{\Delta t}{T}\sum_{n=0}^{N-1}\left|e_q^{n+1}\right|^2\\
&\leq C\sum_{n=0}^{N}\Delta t\big\|\phi_j^n\big\|^2+C\Big\{\big\|\mathbf{u}_j(0)-\mathbf{u}_j^0\big\|^2+\theta\Delta t\big\|\nabla(\mathbf{u}_j(0)-\mathbf{u}_j^0)\big\|^2
\end{aligned}
$$

$$+\Delta t^2\|\mathbf{u}_{j,tt}\|^2_{L^2(0,T;L^2(\Omega))}+\Delta t^2\|\nabla\mathbf{u}_{j,t}\|^2_{L^2(0,T;L^2(\Omega))}$$
$$+\inf_{\mathbf{v}_j^0\in X_h}\left\{\left\|\eta_j^0\right\|^2+\theta\Delta t\left\|\nabla\eta_j^0\right\|^2\right\}+\inf_{\mathbf{v}_j\in X_h}\|\eta_{j,t}\|^2_{L^2(0,T;L^2(\Omega))}$$
$$+\Delta t\inf_{\mathbf{v}_j^n\in X_h}\sum_{n=0}^{N-1}\left\{\left\|\nabla\eta_j^{n+1}\right\|^2+\left\|\nabla\eta_j^n\right\|^2\right\}+C\Delta t^2\Big\}. \tag{3.54}$$

Then, we can further deal with the second to last term of (3.54) as follows:

$$\Delta t\inf_{\mathbf{v}_j^n\in X_h}\sum_{n=0}^{N-1}\left\{\left\|\nabla\eta_j^{n+1}\right\|^2+\left\|\nabla\eta_j^n\right\|^2\right\}\le 2T\max_{n=0,1,\ldots,N}\inf_{\mathbf{v}_j^n\in X_h}\left\|\nabla\eta_j^n\right\|^2.$$

We can finally utilize Gronwall inequality to yield the convergence result (3.22) of A1. □

4. The ensemble algorithm for data-passing scheme

Inspired by [6], we discover that the data-passing scheme offers improved accuracy and stability compared to the IMEX scheme while maintaining unconditional stability and convergence. Therefore, in this section, we will establish two effective ensemble algorithms based on the data-passing scheme for fast-solving the random heat-heat interface-coupled model. We first propose the following ensemble algorithm for the data-passing scheme.

Ensemble algorithm for data-passing scheme (A2)

Let $\Delta t>0$, $\bar\nu_i^n=(\sum_{j=1}^J\nu_{i,j}(\mathbf{x},t^n))/J$, $\kappa_{\max}=\max_j\kappa_j$, $\mathbf{u}_j^0\in X_h$ and $\mathbf{f}_j\in L^2(H^{-1}(\Omega);0,T))$ for $j=1,\ldots,J$. Given $\mathbf{u}_j^n\in X_h$, for $n=0,1,2,\ldots,N-1$ and $i,k=1,2,i\neq k$, we can find $\mathbf{u}_j^{n+1}\in X_h$ by

$$\left(\frac{u_{i,j}^{n+1}-u_{k,j}^n}{\Delta t},v_i\right)+\left(\bar\nu_i^{n+1}\nabla u_{i,j}^{n+1},\nabla v_i\right)+\left((\nu_{i,j}^{n+1}-\bar\nu_i^{n+1})\nabla u_{i,j}^n,\nabla v_i\right)$$
$$+\int_\Gamma\kappa_{\max}\big(u_{i,j}^{n+1}-u_{k,j}^n\big)v_1\mathrm{d}s+\int_\Gamma\left(\kappa_j-\kappa_{\max}\right)\left(u_{i,j}^n-u_{k,j}^n\right)v_1\mathrm{d}s \tag{4.1a}$$
$$=\big(f_{i,j}^{n+1},v_i\big),\quad\forall v_i\in X_{i,h}. \tag{4.1b}$$

The term in the (4.1a) represents a reflection of the data-passing scheme. Such an algorithm has the following unconditional stability.

Theorem 4.1 (A2 Stability)**.** *Suppose that* $\mathbf{f}_j\in L^2(H^{-1}(\Omega);0,T)$, $\mathbf{u}_j^{n+1}\in X_h$ *satisfy* (4.1) *for each* $n\in\{0,1,2,\ldots,N-1\}$*, and the conditions* (3.10)-(3.12) *hold. Then,*

there exists a generic positive constant C independent of $h, \Delta t, J$ *such that* $\mathbf{u}_j^{n+1}$ *satisfies*

$$\begin{aligned}&\left\|\mathbf{u}_j^N\right\|^2+\theta_+\Delta t\left\|\nabla\mathbf{u}_j^N\right\|^2+(\theta-\theta_+)\Delta t\sum_{n=0}^{N-1}\left\|\nabla\mathbf{u}_j^{n+1}\right\|^2+\kappa_{\max}\Delta t\left\|\mathbf{u}_j^N\right\|_\Gamma^2\\&\leq\left\|\mathbf{u}_j^0\right\|^2+C\Delta t\left\|\nabla\mathbf{u}_j^0\right\|^2+C\Delta t\left\|\mathbf{u}_j^0\right\|_\Gamma^2+C\Delta t\sum_{n=0}^{N-1}\left\|\mathbf{f}_j^{n+1}\right\|_{-1}^2.\end{aligned}\tag{4.2}$$

Proof. Taking $\mathbf{v}=2\Delta t\mathbf{u}_j^{n+1}$ in (4.1), we have

$$\begin{aligned}&2\left(\mathbf{u}_j^{n+1}-\mathbf{u}_j^n,\mathbf{u}_j^{n+1}\right)+2\Delta t\left(\bar{\nu}^{n+1}\nabla\mathbf{u}_j^{n+1},\nabla\mathbf{u}_j^{n+1}\right)\\&\quad+2\kappa_{\max}\Delta t\left\|\mathbf{u}_j^{n+1}\right\|_\Gamma^2-2\Delta t\int_\Gamma\kappa_j u_{2,j}^n u_{1,j}^{n+1}\mathrm{d}s\\&\quad-2\Delta t\int_\Gamma\kappa_j u_{1,j}^n u_{2,j}^{n+1}\mathrm{d}s+2\Delta t\int_\Gamma(\kappa_j-\kappa_{\max})u_{1,j}^n u_{1,j}^{n+1}\mathrm{d}s\\&\quad+2\Delta t\int_\Gamma(\kappa_j-\kappa_{\max})u_{2,j}^n u_{2,j}^{n+1}\mathrm{d}s\\&=-2\Delta t\left((\nu_j^{n+1}-\bar{\nu}^{n+1})\nabla\mathbf{u}_j^n,\nabla\mathbf{u}_j^{n+1}\right)+2\Delta t\big(\mathbf{f}_j^{n+1},\mathbf{u}_j^{n+1}\big).\end{aligned}\tag{4.3}$$

Using the Young's inequality,

$$2(a-b,a)=a^2+(a-b)^2-b^2$$

and (3.10), we get

$$\begin{aligned}&\left\|\mathbf{u}_j^{n+1}\right\|^2-\left\|\mathbf{u}_j^n\right\|^2+2\theta\Delta t\left\|\nabla\mathbf{u}_j^{n+1}\right\|^2+2\kappa_{\max}\Delta t\left\|\mathbf{u}_j^{n+1}\right\|_\Gamma^2\\&\leq2\Delta t\int_\Gamma(\kappa_{\max}-\kappa_j)u_{1,j}^n u_{1,j}^{n+1}\mathrm{d}s+2\Delta t\int_\Gamma(\kappa_{\max}-\kappa_j)u_{2,j}^n u_{2,j}^{n+1}\mathrm{d}s\\&\quad+2\Delta t\int_\Gamma\kappa_j u_{2,j}^n u_{1,j}^{n+1}\mathrm{d}s+2\Delta t\int_\Gamma\kappa_j u_{1,j}^n u_{2,j}^{n+1}\mathrm{d}s\\&\quad-2\Delta t\left((\nu_j^{n+1}-\bar{\nu}^{n+1})\nabla\mathbf{u}_j^n,\nabla\mathbf{u}_j^{n+1}\right)+2\Delta t\big(\mathbf{f}_j^{n+1},\mathbf{u}_j^{n+1}\big).\end{aligned}\tag{4.4}$$

Applying the Cauchy-Schwarz and Young's inequalities on the interface terms, we can obtain

$$\begin{aligned}&2\Delta t\int_\Gamma(\kappa_{\max}-\kappa_j)u_{1,j}^n u_{1,j}^{n+1}\mathrm{d}s+2\Delta t\int_\Gamma(\kappa_{\max}-\kappa_j)u_{2,j}^n u_{2,j}^{n+1}\mathrm{d}s\\&\quad+2\Delta t\int_\Gamma\kappa_j u_{2,j}^n u_{1,j}^{n+1}\mathrm{d}s+2\Delta t\int_\Gamma\kappa_j u_{1,j}^n u_{2,j}^{n+1}\mathrm{d}s\\&\leq\kappa_{\max}\Delta t\left\|\mathbf{u}_j^n\right\|_\Gamma^2+\kappa_{\max}\Delta t\left\|\mathbf{u}_j^{n+1}\right\|_\Gamma^2.\end{aligned}\tag{4.5}$$

The estimation of the last two terms at the RHS of (4.4) can be referred to (3.19). Substituting (3.19), (4.5) into (4.4) yields

$$\|\mathbf{u}_j^{n+1}\|^2 - \|\mathbf{u}_j^n\|^2 + 2\Delta t(\theta - \theta_+ - \alpha)\|\nabla \mathbf{u}_j^{n+1}\|^2 + \theta_+ \Delta t \left(\|\nabla \mathbf{u}_j^{n+1}\|^2 - \|\nabla \mathbf{u}_j^n\|^2\right)$$
$$+ \kappa_{\max}\Delta t \left(\|\mathbf{u}_j^{n+1}\|^2 - \|\mathbf{u}_j^n\|^2\right) \le \frac{\Delta t}{2\alpha}\|\mathbf{f}_j^{n+1}\|_{-1}^2. \tag{4.6}$$

With conditions (3.10) and (3.12), summing over $n = 0, 1, \ldots, N-1$, and then choosing $\alpha = (\theta - \theta_+)/2$, we will address

$$\|\mathbf{u}_j^N\|^2 + \theta_+ \Delta t\|\nabla \mathbf{u}_j^N\|^2 + (\theta - \theta_+)\Delta t \sum_{n=0}^{N-1} \|\nabla \mathbf{u}_j^{n+1}\|^2 + \kappa_{\max}\Delta t\|\mathbf{u}_j^N\|^2$$
$$\le \|\mathbf{u}_j^0\|^2 + \theta_+ \Delta t\|\nabla \mathbf{u}_j^0\|^2 + \kappa_{\max}\Delta t\|\mathbf{u}_j^0\|_\Gamma^2 + \frac{\Delta t}{\theta - \theta_+}\|\mathbf{f}_j^{n+1}\|_{-1}^2, \tag{4.7}$$

which completes the stability demonstration of A2. □

Next, we will estimate the approximation error of A2.

Theorem 4.2 (A2 Error Estimate)**.** *Let* $\mathbf{u}_j(t^{n+1})$ *and* $\mathbf{u}_j^{n+1}$ *be the solutions of* (2.14) *and the algorithm A2 at time* t^{n+1}*, respectively. Assume conditions (iii)-(iv) and the stability condition* (3.12) *hold. Then, there exists a generic positive constant C independent of* $h, \Delta t, J$ *for any* $n \in \{0, 1, 2, \ldots, N-1\}$ *such that*

$$\|\mathbf{u}_j(t^N) - \mathbf{u}_j^N\|^2 + \kappa_{\max}\Delta t\|\mathbf{u}_j(t^N) - \mathbf{u}_j^N\|_\Gamma^2$$
$$+ \theta_+ \Delta t\|\nabla \mathbf{u}_j(t^N) - \nabla \mathbf{u}_j^N\|^2 + (\theta - \theta_+)\Delta t \sum_{n=0}^{N-1} \|\nabla \mathbf{u}_j(t^{n+1}) - \nabla \mathbf{u}_j^{n+1}\|^2$$
$$\le C\Big\{ \|\mathbf{u}_j(0) - \mathbf{u}_j^0\|^2 + \kappa_{\max}\Delta t\|\mathbf{u}_j(0) - \mathbf{u}_j^0\|_\Gamma^2 + \theta_+ \Delta t\|\nabla(\mathbf{u}_j(0) - \mathbf{u}_j^0)\|^2$$
$$+ \Delta t^2 \|\nabla \mathbf{u}_{j,t}\|_{L^2(0,T;L^2\Omega)}^2 + \Delta t^2 \|\mathbf{u}_{j,tt}\|_{L^2(0,T;L^2(\Omega))}^2$$
$$+ \inf_{\mathbf{v}_j^0 \in X_h} \left\{ \|\mathbf{u}_j(0) - \mathbf{v}_j^0\|^2 + \kappa_{\max}\Delta t\|\nabla(\mathbf{u}_j(0) - \mathbf{v}_j^0)\|_\Gamma^2 \right\}$$
$$+ \inf_{\mathbf{v}_j \in X_h} \|(\mathbf{u}_j(t^n) - \mathbf{v}_j^n)_t\|_{L^2(0,T;L^2(\Omega))}^2$$
$$+ T \max_{n=0,1,\ldots,N} \inf_{\mathbf{v}_j^n \in X_h} \|\nabla(\mathbf{u}_j(t^n) - \mathbf{v}_j^n)\|^2 \Big\}. \tag{4.8}$$

Proof. Restricting test function $\mathbf{v}$ to X_h and subtracting (4.1) from (2.14), we can derive the following error equation by the similar way of (3.23):

$$(\mathbf{r}^{n+1}, \mathbf{v}) + \left(\frac{\mathbf{u}_j(t^{n+1}) - \mathbf{u}_j^{n+1}}{\Delta t} - \frac{\mathbf{u}_j(t^n) - \mathbf{u}_j^n}{\Delta t}, \mathbf{v} \right)$$
$$+ \left(\bar{\nu}^{n+1}(\nabla \mathbf{u}_j(t^{n+1}) - \nabla \mathbf{u}_j^{n+1}), \nabla \mathbf{v} \right)$$
$$+ \left((\nu_j^{n+1} - \bar{\nu}^{n+1})(\nabla \mathbf{u}_j(t^n) - \nabla \mathbf{u}_j^n), \nabla \mathbf{v} \right)$$

$$
\begin{aligned}
&+\Big((\nu_j^{n+1}-\bar{\nu}^{n+1})(\nabla\mathbf{u}_j(t^{n+1})-\nabla\mathbf{u}_j(t^n)),\nabla\mathbf{v}\Big)\\
&+\int_\Gamma \kappa_j\left(u_{1,j}(t^{n+1})-u_{2,j}(t^{n+1})\right)v_1\mathrm{d}s\\
&+\int_\Gamma \kappa_j\left(u_{2,j}(t^{n+1})-u_{1,j}(t^{n+1})\right)v_2\mathrm{d}s\\
&-\int_\Gamma \kappa_{\max}\big(u_{1,j}^{n+1}-u_{2,j}^{n}\big)v_1\mathrm{d}s-\int_\Gamma \kappa_{\max}\big(u_{2,j}^{n+1}-u_{1,j}^{n}\big)v_2\mathrm{d}s\\
&-\int_\Gamma \big(\kappa_j-\kappa_{\max}\big)\big(u_{1,j}^{n}-u_{2,j}^{n}\big)v_1\mathrm{d}s-\int_\Gamma \big(\kappa_j-\kappa_{\max}\big)\big(u_{2,j}^{n}-u_{1,j}^{n}\big)v_2\mathrm{d}s=0. \quad (4.9)
\end{aligned}
$$

For the interface terms of (4.9), we skillfully add and subtract four terms

$$
\begin{aligned}
&\int_\Gamma \kappa_{\max}\left(u_1(t^{n+1})-u_2(t^n)\right)\phi_{1,j}^{n+1}\mathrm{d}s,\\
&\int_\Gamma \kappa_{\max}\left(u_2(t^{n+1})-u_1(t^n)\right)\phi_{2,j}^{n+1}\mathrm{d}s,\\
&\int_\Gamma \big(\kappa_j-\kappa_{\max}\big)\big(u_1(t^n)-u_2(t^n)\big)\phi_{1,j}^{n+1}\mathrm{d}s,\\
&\int_\Gamma \big(\kappa_j-\kappa_{\max}\big)\big(u_2(t^n)-u_1(t^n)\big)\phi_{2,j}^{n+1}\mathrm{d}s
\end{aligned}
$$

to maintain first order accuracy in time.

$$
\begin{aligned}
&\int_\Gamma \kappa_j\left(u_{1,j}(t^{n+1})-u_{2,j}(t^{n+1})\right)\phi_{1,j}^{n+1}\mathrm{d}s+\int_\Gamma \kappa_j\left(u_{2,j}(t^{n+1})-u_{1,j}(t^{n+1})\right)\phi_{2,j}^{n+1}\mathrm{d}s\\
&\quad-\int_\Gamma \kappa_{\max}\big(u_{1,j}^{n+1}-u_{2,j}^{n}\big)\phi_{1,j}^{n+1}\mathrm{d}s-\int_\Gamma \kappa_{\max}\big(u_{2,j}^{n+1}-u_{1,j}^{n}\big)\phi_{2,j}^{n+1}\mathrm{d}s\\
&\quad-\int_\Gamma \big(\kappa_j-\kappa_{\max}\big)\big(u_{1,j}^{n}-u_{2,j}^{n}\big)\phi_{1,j}^{n+1}\mathrm{d}s-\int_\Gamma \big(\kappa_j-\kappa_{\max}\big)\big(u_{2,j}^{n}-u_{1,j}^{n}\big)\phi_{2,j}^{n+1}\mathrm{d}s\\
=&\int_\Gamma \kappa_{\max}\big(\mathbf{u}_j(t^{n+1})-\mathbf{u}_j^{n+1}\big)\phi_j^{n+1}\mathrm{d}s+\int_\Gamma \big(\kappa_j-\kappa_{\max}\big)\big(\mathbf{u}_j(t^n)-\mathbf{u}_j^{n}\big)\phi_j^{n+1}\mathrm{d}s\\
&\quad-\int_\Gamma \kappa_j\big(u_{2,j}(t^n)-u_{2,j}^{n}\big)\phi_{1,j}^{n+1}\mathrm{d}s-\int_\Gamma \kappa_j\big(u_{1,j}(t^n)-u_{1,j}^{n}\big)\phi_{2,j}^{n+1}\mathrm{d}s\\
&\quad+\int_\Gamma \big(\kappa_j-\kappa_{\max}\big)\big(\mathbf{u}_j(t^{n+1})-\mathbf{u}_j(t^n)\big)\phi_j^{n+1}\mathrm{d}s\\
&\quad-\int_\Gamma \kappa_j\big(u_{2,j}(t^{n+1})-u_{2,j}(t^n)\big)\phi_{1,j}^{n+1}\mathrm{d}s-\int_\Gamma \kappa_j\big(u_{1,j}(t^{n+1})-u_{1,j}(t^n)\big)\phi_{2,j}^{n+1}\mathrm{d}s. \quad (4.10)
\end{aligned}
$$

Choosing $\mathbf{v}=\phi_j^{n+1}$, substituting (4.10) into (4.9), we can conclude

$$
\begin{aligned}
&\frac{1}{2\Delta t}\left(\left\|\phi_j^{n+1}\right\|^2-\left\|\phi_j^{n}\right\|^2\right)+\theta\left\|\nabla\phi_j^{n+1}\right\|^2+\kappa_{\max}\left\|\phi_j^{n+1}\right\|_\Gamma^2\\
&\le-\frac{1}{\Delta t}\big(\eta_j^{n+1}-\eta_j^n,\phi_j^{n+1}\big)-\big(\mathbf{r}_j^{n+1},\phi_j^{n+1}\big)-\Big((\nu_j^{n+1}-\bar{\nu}^{n+1})\nabla\phi_j^n,\nabla\phi_j^{n+1}\Big)
\end{aligned}
$$

$$
\begin{aligned}
&- \left(\bar{\nu}^{n+1}\nabla\eta_j^{n+1}, \nabla\phi_j^{n+1}\right) - \left((\nu_j^{n+1} - \bar{\nu}^{n+1})\nabla\eta_j^n, \nabla\phi_j^{n+1}\right) \\
&- \left((\nu_j^{n+1} - \bar{\nu}^{n+1})(\nabla\mathbf{u}_j(t^{n+1}) - \nabla\mathbf{u}_j(t^n)), \nabla\phi_j^{n+1}\right) \\
&+ \int_\Gamma \kappa_j \left(u_{2,j}(t^{n+1}) - u_{2,j}(t^n)\right) \phi_{1,j}^{n+1}\mathrm{d}s \\
&+ \int_\Gamma \kappa_j \left(u_{1,j}(t^{n+1}) - u_{1,j}(t^n)\right) \phi_{2,j}^{n+1}\mathrm{d}s \\
&+ \int_\Gamma \big(\kappa_{\max} - \kappa_j\big)\big(\mathbf{u}_j(t^{n+1}) - \mathbf{u}_j(t^n)\big)\phi_j^{n+1}\mathrm{d}s \\
&+ \int_\Gamma \big(\kappa_{\max} - \kappa_j\big)\big(\mathbf{u}_j(t^n) - \mathbf{u}_j^n\big)\phi_j^{n+1}\mathrm{d}s \\
&+ \int_\Gamma \kappa_j\big(u_{2,j}(t^n) - u_{2,j}^n\big)\phi_{1,j}^{n+1}\mathrm{d}s \\
&+ \int_\Gamma \kappa_j\big(u_{1,j}(t^n) - u_{1,j}^n\big)\phi_{2,j}^{n+1}\mathrm{d}s - \int_\Gamma \kappa_{\max}\eta_j^{n+1}\phi_j^{n+1}\mathrm{d}s. \qquad (4.11)
\end{aligned}
$$

Next, we need to bound the terms on the RHS of (4.11). The estimation of the first six items can be referred to (3.25)-(3.30). For the interface terms, utilizing the trace theorem and Young's inequality, we get

$$
\begin{aligned}
&\int_\Gamma \kappa_j \left(u_{2,j}(t^{n+1}) - u_{2,j}(t^n)\right) \phi_{1,j}^{n+1}\mathrm{d}s + \int_\Gamma \kappa_j \left(u_{1,j}(t^{n+1}) - u_{1,j}(t^n)\right) \phi_{2,j}^{n+1}\mathrm{d}s \\
&\le \frac{C_t^4\kappa_j^2}{2\epsilon_1}\big\|\nabla(\mathbf{u}_j(t^{n+1}) - \mathbf{u}_j(t^n))\big\|^2 + \frac{\epsilon_1}{2}\big\|\nabla\phi_j^{n+1}\big\|^2, \qquad (4.12) \\
&\int_\Gamma \big(\kappa_{\max} - \kappa_j\big)\big(\mathbf{u}_j(t^{n+1}) - \mathbf{u}_j(t^n)\big)\phi_j^{n+1}\mathrm{d}s \\
&\le \frac{C_t^4(\kappa_{\max} - \kappa_j)^2}{2\epsilon_2}\big\|\nabla(\mathbf{u}_j(t^{n+1}) - \mathbf{u}_j(t^n))\big\|^2 + \frac{\epsilon_2}{2}\big\|\nabla\phi_j^{n+1}\big\|^2, \qquad (4.13) \\
&\int_\Gamma \big(\kappa_{\max} - \kappa_j\big)\big(\eta_j^n + \phi_j^n\big)\phi_j^{n+1}\mathrm{d}s \\
&\le \frac{\kappa_{\max} - \kappa_j}{2}\big\|\phi_j^n\big\|_\Gamma^2 + \frac{\kappa_{\max} - \kappa_j}{2}\big\|\phi_j^{n+1}\big\|_\Gamma^2 + \frac{C_t^4(\kappa_{\max} - \kappa_j)^2}{2\epsilon_3}\big\|\nabla\eta_j^n\big\|^2 \\
&\quad + \frac{\epsilon_3}{2}\big\|\nabla\phi_j^{n+1}\big\|^2, \qquad (4.14) \\
&\int_\Gamma \kappa_j\big(\eta_{2,j}^n + \phi_{2,j}^n\big)\phi_{1,j}^{n+1}\mathrm{d}s + \int_\Gamma \kappa_j\big(\eta_{1,j}^n + \phi_{1,j}^n\big)\phi_{2,j}^{n+1}\mathrm{d}s \\
&\le \frac{\kappa_j}{2}\big\|\phi_j^n\big\|_\Gamma^2 + \frac{\kappa_j}{2}\big\|\phi_j^{n+1}\big\|_\Gamma^2 + \frac{C_t^4\kappa_j^2}{2\epsilon_4}\big\|\nabla\eta_j^n\big\|^2 + \frac{\epsilon_4}{2}\big\|\nabla\phi_j^{n+1}\big\|^2, \qquad (4.15) \\
&\int_\Gamma \kappa_{\max}\eta_j^{n+1}\phi_j^{n+1}\mathrm{d}s \le \frac{C_t^4\kappa_{\max}^2}{2\epsilon_5}\big\|\nabla\eta_j^{n+1}\big\|^2 + \frac{\epsilon_5}{2}\big\|\nabla\phi_j^{n+1}\big\|^2. \qquad (4.16)
\end{aligned}
$$

For the estimation of other terms at the RHS of (4.11), we can refer to Theorem 3.2. Taking

$$\xi_1 = \frac{2\beta\theta_+}{10|\bar{\nu}^{n+1}|_\infty}, \quad \xi_2 = 1, \quad \xi_3 = \xi_4 = \frac{2\beta}{10}, \quad \xi_5 = \xi_6 = \frac{2\beta\theta_+}{10}$$

in Theorem 3.2, where β is a positive constant

$$\epsilon_1 = \epsilon_2 = \epsilon_3 = \epsilon_4 = \epsilon_5 = \frac{2\beta\theta_+}{10},$$

we have

$$\begin{aligned}
&\frac{1}{2\Delta t}\left(\|\phi_j^{n+1}\|^2 - \|\phi_j^n\|^2\right) + \frac{\theta_+}{2}\left(\|\nabla\phi_j^{n+1}\|^2 - \|\nabla\phi_j^n\|^2\right) \\
&\quad + \big(\theta - (1+\beta)\theta_+\big)\|\nabla\phi_j^{n+1}\|^2 + \frac{\kappa_{\max}}{2}\left(\|\phi_j^{n+1}\|_\Gamma^2 - \|\phi_j^n\|_\Gamma^2\right) \\
\le\ & \frac{C|\bar{\nu}^{n+1}|_\infty^2}{\beta\theta_+}\|\nabla\eta_j^{n+1}\|^2 + \frac{C\kappa_{\max}^2}{\beta\theta_+}\|\nabla\eta_j^{n+1}\|^2 + \frac{C\theta_+}{\beta}\|\nabla\eta_j^n\|^2 + \frac{C\kappa_j^2}{\beta\theta_+}\|\nabla\eta_j^n\|^2 \\
&\quad + \frac{C(\kappa_{\max}-\kappa_j)^2}{\beta\theta_+}\|\nabla\eta_j^n\|^2 + \frac{C\theta_+}{\beta}\|\nabla(\mathbf{u}_j(t^{n+1}) - \mathbf{u}_j(t^n))\|^2 \\
&\quad + \frac{C\kappa_j^2}{\beta\theta_+}\|\nabla(\mathbf{u}_j(t^{n+1}) - \mathbf{u}_j(t^n))\|^2 + \frac{C(\kappa_{\max}-\kappa_j)^2}{\beta\theta_+}\|\nabla(\mathbf{u}_j(t^{n+1}) - \mathbf{u}_j(t^n))\|^2 \\
&\quad + \frac{C}{\beta\theta_+}\|\mathbf{r}_j^{n+1}\|^2 + \frac{C}{\beta\theta_+}\left\|\frac{\eta_j^{n+1} - \eta_j^n}{\Delta t}\right\|^2.
\end{aligned} \tag{4.17}$$

The selection of β is similar to the selection of α in Theorem 3.2. Setting $\beta = (\theta - \theta_+)/2\theta_+$, we have

$$\theta - (1+\beta)\theta_+ > \frac{\theta - \theta_+}{2} > 0$$

based on the upper bound in condition (3.11) and the stability condition (3.12). The rest of the detailed analysis is similar to Theorem 3.2, and the final result can be derived as follows:

$$\begin{aligned}
&\|\phi_j^N\|^2 + \kappa_{\max}\Delta t\|\phi_j^N\|_\Gamma^2 + (\theta - \theta_+)\Delta t\sum_{n=0}^{N-1}\|\nabla\phi_j^{n+1}\|^2 + \theta_+\Delta t\|\nabla\phi_j^N\|^2 \\
\le\ & C\Big\{\|\mathbf{u}_j(0) - \mathbf{u}_j^0\|^2 + \kappa_{\max}\Delta t\|\mathbf{u}_j(0) - \mathbf{u}_j^0\|_\Gamma^2 + \theta_+\Delta t\|\nabla(\mathbf{u}_j(0) - \mathbf{u}_j^0)\|^2 \\
&\quad + \Delta t^2\|\nabla\mathbf{u}_{j,t}\|_{L^2(0,T;L^2\Omega)}^2 + \Delta t^2\|\mathbf{u}_{j,tt}\|_{L^2(0,T;L^2(\Omega))}^2 \\
&\quad + \inf_{\mathbf{v}_j^0\in X_h}\left\{\|\eta_j^0\|^2 + \kappa_{\max}\Delta t\|\eta_j^0\|_\Gamma^2\right\} + \inf_{\mathbf{v}_j\in X_h}\|\eta_{j,t}\|_{L^2(0,T;L^2(\Omega))}^2 \\
&\quad + \Delta t\inf_{\mathbf{v}_j^n\in X_h}\sum_{n=0}^{N-1}\left\{\|\nabla\eta_j^{n+1}\|^2 + \|\nabla\eta_j^n\|^2\right\}\Big\},
\end{aligned} \tag{4.18}$$

where C is a generic positive constant independent of $h, \Delta t$, and J. By the triangle inequality, we arrive at the final result (4.8). □

Note that the core idea of the ensemble method in the A2 algorithm is to compute the expectation of diffusion coefficient $\bar{\nu}_i^n$ at each time step. Interestingly, we can further optimize the A2 algorithm by taking the temporal average of $\nu_{i,j}(\mathbf{x}, t^n)$ as well. This way, we can obtain several linear equations that have the same coefficient matrix not only across samples but also across time steps, which can significantly reduce the storage demand and the computational cost. The optimized algorithm is presented as follows.

Optimize Ensemble Algorithm for Data-passing scheme (A3)

Let $\Delta t > 0$, $\bar{\nu}_i = \frac{1}{N}\sum_{n=1}^{N} \bar{\nu}_i^n$, $\mathbf{u}_j^0 \in X_h$ and $\mathbf{f}_j \in L^2(H^{-1}(\Omega); 0, T))$ for $j = 1, \ldots, J$. Given $\mathbf{u}_j^n \in X_h$, for $n = 0, 1, 2, \ldots, N-1$ and $i, k = 1, 2, 1 \neq k$, we will find $\mathbf{u}_j^{n+1} \in X_h$ by

$$\begin{aligned}
&\left(\frac{u_{i,j}^{n+1} - u_{i,j}^n}{\Delta t}, v_i\right) + \left(\bar{\nu}_i \nabla u_{i,j}^{n+1}, \nabla v_i\right) + \left((\nu_{i,j}^{n+1} - \bar{\nu}_i)\nabla u_{i,j}^n, \nabla v_i\right) \\
&\quad + \int_\Gamma \kappa_{\max}\left(u_{i,j}^{n+1} - u_{i,j}^n\right) v_1 \mathrm{d}s + \int_\Gamma \left(\kappa_j - \kappa_{\max}\right)\left(u_{i,j}^n - u_{k,j}^n\right) v_1 \mathrm{d}s \\
&= \left(f_{i,j}^{n+1}, v_1\right), \quad \forall v_i \in X_{i,h}.
\end{aligned} \tag{4.19}$$

The proof for the stability and the convergence of A3 is similar to A2, and the parameter condition $\theta > \theta_+$ is also required for A3.

Remark 4.1. We proposed the A2 for the heat-heat interface-coupled problem with three random coefficients, which are more complex than the single domain random problem [23]. Fortunately, compared with the results of [23], we do not need to strengthen or impose any constraint conditions to obtain unconditional stability and convergence. The existing ensemble algorithms in [12–15, 23–25] all rely on a small perturbation assumption. However, due to the special nature of the friction parameter κ as a random function independent of time and space, both proposed algorithms can avoid this assumption as shown in the above analysis and in [15, Section 4]. To further indicate this advantage, we also test the κ from 10^{-2} to 10^{1} in the numerical experiments, which is usually between 10^{-3} and 10^{3}. Moreover, if the time and space maximum of the diffusion coefficient $\nu_{i,j}(\mathbf{x}, t)$ can be easily identified, the parameter condition $\theta > \theta_+$ of both proposed algorithms is not necessary. This also suggests that if the random parameter has a large perturbation, we can use the maximum value or L^∞ norm of the random parameter as the key of the ensemble method.

Remark 4.2. This paper presents three algorithms for solving heat-heat model with three random parameters. We compare the structure and complexity of these algorithms and show that A3 algorithm is the most efficient one. The algorithm is proposed based on the logical rigor of the algorithm construction, which is gradually advanced. We also aim to apply the idea of A3 algorithm to other time-dependent stochastic problems.

5. Numerical experiments

In this section, we conduct three numerical experiments to demonstrate the accuracy and efficiency of the proposed ensemble algorithms for the interface-coupled system with three random coefficients. The first experiment involves a smooth problem to verify the convergence of the three proposed ensemble methods. We also measure the CPU time to compare the performance of our methods. The second experiment examines the energy dissipation results of the three algorithms to show that the proposed methods are unconditionally stable. The third experiment simulates a random steel-titanium composite plate fuel cell 3D model to illustrate the combination of our ensemble algorithms and the Monte Carlo method, and further observe its internal heat conduction behavior. In all experiments, we use linear Lagrangian elements (P1) to construct the finite element spaces. We implement all the numerical experiments using the open software FreeFEM++ [9].

5.1. Smooth problem

In the first numerical experiment, we test a smooth problem with an exact solution adapted from [6] to check the convergence rate of our ensemble algorithms. Assume that $\Omega_1 = [0,1]\times[0,1]$, $\Omega_2 = [0,1]\times[-1,0]$, the interface Γ of the current computational domain is the portion of the x-axis from 0 to 1, $\hat{n}_1 = [0,-1]^T$ and $\hat{n}_2 = [0,1]^T$. The exact solution is selected as follows:

$$u_1(t,x,y) = ax(1-x)(1-y)e^{-t},$$
$$u_2(t,x,y) = ax(1-x)(c_1 + c_2 y + c_3 y^2)e^{-t},$$

which also determines the Dirichlet boundary condition, initial condition, and source terms of this smooth problem. The selection of above constants c_1, c_2, c_3 should be determined by (2.1)-(2.4). Inspired by [6], we can choose

$$c_1 = 1 + \frac{\nu_1}{\kappa}, \quad c_2 = \frac{-\nu_1}{\nu_2}, \quad c_3 = c_2 - c_1.$$

In order to obtain not only the optimal convergence order of the error H^1-norm but also that of L^2-norm, we uniformly refine the mesh size h from $1/8$ to $1/32$ and make the time step size $\Delta t = h^2$. We also introduced an error notation $e_{u_i} = u_i(t^N) - u_i^N$ with $T = 1.0,\ N = T/\Delta t$ to display the results conveniently.

We first consider the smooth heat-heat interface-coupled model with two random diffusion coefficients ν_1, ν_2 and one random friction parameter κ. We select a group of simulation with $J \times J, J = 3$ members to test the convergence performance of A1 and A2 algorithms, including three friction parameters $\kappa_1 = 0.01, \kappa_2 = 1.0, \kappa_3 = 10.0$, and three diffusion coefficient groups

$$\nu_{1,j}(\mathbf{x},t) = \nu_{2,j}(\mathbf{x},t) = 1 + (1+\varepsilon_j)\sin(t)$$

with $\varepsilon_1 = 0.6207, \varepsilon_2 = 0.1841$ and $\varepsilon_3 = 0.2691$ [23]. The parameter a can be taken as 1.0. The approximate accuracy of the u_1 and u_2 in L^2-norm and H^1-norm of the A1 algorithm are shown in Tables 1 and 2, which can verify the optimal convergence orders for both u_1 and u_2. Numerical results for A2 in Tables 3 and 4 show the L^2-norm and H^1-norm of u_1 and u_2, and also achieve the optimal convergence order. Both results can indicate the effectiveness of our algorithms and confirm the theoretical analysis.

Table 1: The L^2-error of u_1 and u_2 for A1 $(J \times J, J = 3)$ with different κ_j and ν_j while $\Delta t = h^2$.

h	$\|e_{u_1}\|^{\kappa_1,\nu_1}$	$\|e_{u_1}\|^{\kappa_1,\nu_2}$	$\|e_{u_1}\|^{\kappa_1,\nu_3}$	$\|e_{u_1}\|^{\kappa_2,\nu_1}$	$\|e_{u_1}\|^{\kappa_2,\nu_2}$	$\|e_{u_1}\|^{\kappa_2,\nu_3}$	$\|e_{u_1}\|^{\kappa_3,\nu_1}$	$\|e_{u_1}\|^{\kappa_3,\nu_2}$	$\|e_{u_1}\|^{\kappa_3,\nu_3}$
1/8	0.029425	0.026852	0.027425	0.025598	0.022981	0.023555	0.061485	0.049583	0.051935
1/16	0.007428	0.006774	0.006919	0.006439	0.005774	0.005920	0.005812	0.005226	0.005353
1/32	0.001861	0.001697	0.001734	0.001612	0.001445	0.001482	0.001454	0.001307	0.001339
h	$\|e_{u_2}\|^{\kappa_1,\nu_1}$	$\|e_{u_2}\|^{\kappa_1,\nu_2}$	$\|e_{u_2}\|^{\kappa_1,\nu_3}$	$\|e_{u_2}\|^{\kappa_2,\nu_1}$	$\|e_{u_2}\|^{\kappa_2,\nu_2}$	$\|e_{u_2}\|^{\kappa_2,\nu_3}$	$\|e_{u_2}\|^{\kappa_3,\nu_1}$	$\|e_{u_2}\|^{\kappa_3,\nu_2}$	$\|e_{u_2}\|^{\kappa_3,\nu_3}$
1/8	0.025686	0.024358	0.024672	0.026271	0.024784	0.025129	0.019170	0.018401	0.018544
1/16	0.006466	0.006126	0.006206	0.006617	0.006238	0.006326	0.007176	0.006691	0.006801
1/32	0.001619	0.001534	0.001554	0.001657	0.001562	0.001584	0.001798	0.001676	0.001703

Table 2: The H^1-error of u_1 and u_2 for A1 $(J \times J, J = 3)$ with different κ_j and ν_j while $\Delta t = h^2$.

h	$\|e_{u_1}\|^{\kappa_1,\nu_1}$	$\|e_{u_1}\|^{\kappa_1,\nu_2}$	$\|e_{u_1}\|^{\kappa_1,\nu_3}$	$\|e_{u_1}\|^{\kappa_2,\nu_1}$	$\|e_{u_1}\|^{\kappa_2,\nu_2}$	$\|e_{u_1}\|^{\kappa_2,\nu_3}$	$\|e_{u_1}\|^{\kappa_3,\nu_1}$	$\|e_{u_1}\|^{\kappa_3,\nu_2}$	$\|e_{u_1}\|^{\kappa_3,\nu_3}$
1/8	0.154409	0.154317	0.154332	0.154278	0.154284	0.154277	0.161680	0.157971	0.158606
1/16	0.077441	0.077429	0.077431	0.077424	0.077425	0.077424	0.077427	0.077435	0.077433
1/32	0.038750	0.038749	0.038749	0.038748	0.038748	0.038748	0.038749	0.038750	0.038749
h	$\|e_{u_2}\|^{\kappa_1,\nu_1}$	$\|e_{u_2}\|^{\kappa_1,\nu_2}$	$\|e_{u_2}\|^{\kappa_1,\nu_3}$	$\|e_{u_2}\|^{\kappa_2,\nu_1}$	$\|e_{u_2}\|^{\kappa_2,\nu_2}$	$\|e_{u_2}\|^{\kappa_2,\nu_3}$	$\|e_{u_2}\|^{\kappa_3,\nu_1}$	$\|e_{u_2}\|^{\kappa_3,\nu_2}$	$\|e_{u_2}\|^{\kappa_3,\nu_3}$
1/8	0.153415	0.153413	0.153412	0.155123	0.155351	0.155300	0.160554	0.160076	0.160151
1/16	0.076912	0.076913	0.076913	0.077782	0.077902	0.077876	0.079620	0.079709	0.079691
1/32	0.038482	0.038483	0.038482	0.038919	0.038980	0.0389669	0.039842	0.039888	0.039878

Table 3: The L^2-error of u_1 and u_2 for A2 $(J \times J, J = 3)$ with different κ_j and ν_j while $\Delta t = h^2$.

h	$\|e_{u_1}\|^{\kappa_1,\nu_1}$	$\|e_{u_1}\|^{\kappa_1,\nu_2}$	$\|e_{u_1}\|^{\kappa_1,\nu_3}$	$\|e_{u_1}\|^{\kappa_2,\nu_1}$	$\|e_{u_1}\|^{\kappa_2,\nu_2}$	$\|e_{u_1}\|^{\kappa_2,\nu_3}$	$\|e_{u_1}\|^{\kappa_3,\nu_1}$	$\|e_{u_1}\|^{\kappa_3,\nu_2}$	$\|e_{u_1}\|^{\kappa_3,\nu_3}$
1/8	0.015217	0.013336	0.013488	0.014818	0.013350	0.013408	0.014019	0.013540	0.013416
1/16	0.003791	0.003331	0.003367	0.003698	0.003334	0.003349	0.003503	0.003371	0.003345
1/32	0.000947	0.000832	0.000841	0.000924	0.000833	0.000837	0.000875	0.000842	0.000835
h	$\|e_{u_2}\|^{\kappa_1,\nu_1}$	$\|e_{u_2}\|^{\kappa_1,\nu_2}$	$\|e_{u_2}\|^{\kappa_1,\nu_3}$	$\|e_{u_2}\|^{\kappa_2,\nu_1}$	$\|e_{u_2}\|^{\kappa_2,\nu_2}$	$\|e_{u_2}\|^{\kappa_2,\nu_3}$	$\|e_{u_2}\|^{\kappa_3,\nu_1}$	$\|e_{u_2}\|^{\kappa_3,\nu_2}$	$\|e_{u_2}\|^{\kappa_3,\nu_3}$
1/8	0.020930	0.018640	0.019149	0.021187	0.018945	0.019430	0.022571	0.020060	0.020590
1/16	0.005241	0.004663	0.004790	0.005329	0.004768	0.004889	0.005706	0.005078	0.005211
1/32	0.001310	0.001166	0.001198	0.001334	0.001194	0.001224	0.001430	0.001273	0.001306

Table 4: The H^1-error of u_1 and u_2 for A2 $(J \times J, J = 3)$ with different κ_j and ν_j while $\Delta t = h^2$.

h	$\|e_{u_1}\|^{\kappa_1,\nu_1}_{X_1}$	$\|e_{u_1}\|^{\kappa_1,\nu_2}_{X_1}$	$\|e_{u_1}\|^{\kappa_1,\nu_3}_{X_1}$	$\|e_{u_1}\|^{\kappa_2,\nu_1}_{X_1}$	$\|e_{u_1}\|^{\kappa_2,\nu_2}_{X_1}$	$\|e_{u_1}\|^{\kappa_2,\nu_3}_{X_1}$	$\|e_{u_1}\|^{\kappa_3,\nu_1}_{X_1}$	$\|e_{u_1}\|^{\kappa_3,\nu_2}_{X_1}$	$\|e_{u_1}\|^{\kappa_3,\nu_3}_{X_1}$
1/8	0.155245	0.156257	0.155996	0.155376	0.156414	0.156150	0.155754	0.156782	0.156529
1/16	0.077550	0.077678	0.077645	0.077566	0.077695	0.077663	0.077612	0.077738	0.077707
1/32	0.038764	0.038781	0.038776	0.038766	0.038782	0.038778	0.038772	0.038788	0.038784
h	$\|e_{u_2}\|^{\kappa_1,\nu_1}_{X_2}$	$\|e_{u_2}\|^{\kappa_1,\nu_2}_{X_2}$	$\|e_{u_2}\|^{\kappa_1,\nu_3}_{X_2}$	$\|e_{u_2}\|^{\kappa_2,\nu_1}_{X_2}$	$\|e_{u_2}\|^{\kappa_2,\nu_2}_{X_2}$	$\|e_{u_2}\|^{\kappa_2,\nu_3}_{X_2}$	$\|e_{u_2}\|^{\kappa_3,\nu_1}_{X_2}$	$\|e_{u_2}\|^{\kappa_3,\nu_2}_{X_2}$	$\|e_{u_2}\|^{\kappa_3,\nu_3}_{X_2}$
1/8	0.153796	0.154052	0.153984	0.155343	0.155799	0.155690	0.158884	0.159270	0.159178
1/16	0.077033	0.077081	0.077069	0.077811	0.077959	0.077926	0.079638	0.079755	0.079730
1/32	0.038533	0.038546	0.038543	0.038922	0.038987	0.038973	0.039844	0.039893	0.039883

To verify Remark 4.1, we focus on the case where only the friction coefficient κ is a random variable. We conduct a series of simulations with $J = 3$, where the friction parameter is selected as $\kappa_1 = 0.01, \kappa_2 = 1.0, \kappa_3 = 10.0$. All the other physical parameters a, ν_1, ν_2 are set to 1.0. We apply the A2 algorithm to simulate the above case and show the convergence order of the L^2-norm and H^1-norm for two regions in Fig. 2. As can be seen from Fig. 2, the L^2 relative errors and H^1 relative errors of u_1 and u_2 for each sample have attained the optimal convergence order. It is worth noting that the random friction parameter κ we select is not subject to a small perturbation constraint, which positively supports our advantage mentioned in Remark 4.1.

To estimate the uncertainty and sensitivity of the solutions for random PDEs more accurately, we need to use more samples, which may increase the computational cost. Therefore, we compare the computational efficiency of our proposed algorithms with the standard data-passing partitioned algorithm [6] for different numbers of realizations $J \times J, J = 1, 5, 10, 15, 20$. Herein, for simplicity, the two random diffusion coefficients can be selected as

$$\nu_1(\omega, \mathbf{x}, t) = \nu_2(\omega, \mathbf{x}, t) = 1 + (1 + \omega)\sin(t)$$

and the random friction parameter can be defined as $\kappa(\omega) = 0.01 + \omega$. The comparison of the elapsed CPU times is shown in Table 5, which indicates that the proposed ensemble methods are significantly faster than the standard data-passing partitioned non-ensemble method except for the case $J \times J = 1 \times 1$. More importantly, both methods capture the same behaviors while the A1 saves about 90.5% of the computation

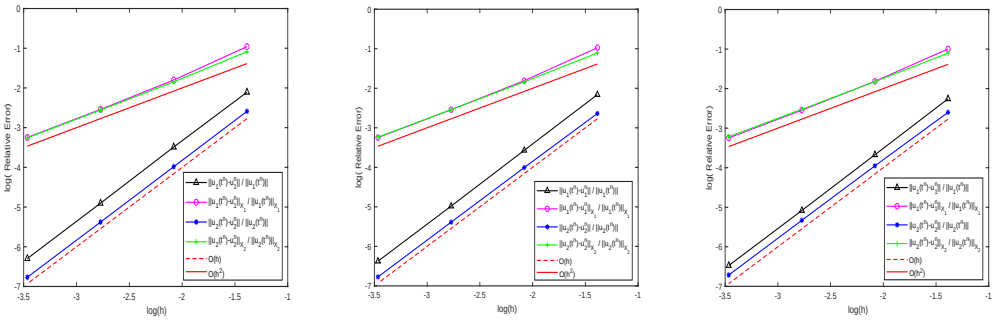

(a) $\kappa_1 = 0.01$ (b) $\kappa_2 = 1.0$ (c) $\kappa_3 = 10.0$

Figure 2: The L^2-error and H^1-error of the u_1 and u_2 for A2 (J=3) with different κ_j.

Table 5: The comparison of the elapsed CPU time while the mesh size $h = 1/32$.

$J \times J$	1×1	5×5	10×10	15×15	20×20
Standard Data-passing Partitioned	151.2	3793.4	15334.6	34203.5	60993.0
A1	159.9	674.6	1920.5	3997.7	5737.8
A2	157.9	442.4	1371.6	2886.5	4972.2
A3	12.8	301.1	1198.5	2692.9	4801.8

time, the A2 saves about 91.8% of the computation time, and the A3 saves about 92.1% of the computation time with $J \times J = 20 \times 20$. Note that due to the fact that the SAV method doubles the number of equations, the A1 algorithm takes more CPU time than the A2. Moreover, the elapsed CPU time of the A3 algorithm is not much less than that of A2. That is because the A3 algorithm only calculates the temporal average of $\nu_{i,j}$ on top of the A2 algorithm. Clearly, the CPU time for calculating more N linear systems is not much longer than $J \times J$. Thus, we can verify the superiority of our proposed algorithms by comparing the CPU times.

5.2. Stability problem

In the second numerical experiment, we test the stability of the proposed ensemble algorithms, especially unconditional stability. For simplicity, we can set $f_{i,j} = 0$, $u_{i,j}^0 = 1.0$, and $u_{i,j} = 0$ on Γ_i based on the domain and parameter selections $\nu_1(\omega, \mathbf{x}, t), \nu_2(\omega, \mathbf{x}, t)$ and $\kappa(\omega)$ of the first numerical experiment. Fig. 3(a) displays the quantity of energy $0.5 * \|u_1^{n+1}\|^2 + 0.5 * \|u_2^{n+1}\|^2$ on large time step points $\Delta t = 0.1$ while $h = 1/32$, where

$$u_i^{n+1} = \frac{1}{J \times J} \sum_{j=1}^{J \times J} u_{i,j}^{n+1}.$$

We can easily calculate that the energy equals 1 while $t = 0$. It is clear to see that the energy of both algorithms decreases rapidly and finally reaches a stable state.

It is known that SAV is a approach to deal with stiff problems in order to use a relative large time step size. Therefore, to test the superiority of the SAV in achieving unconditional stability, we conducted test by excluding the SAV from the A1 algorithm. Fig. 3(b) illustrate the evolution of $0.5 * \|u_1^{n+1}\|^2 + 0.5 * \|u_2^{n+1}\|^2$ in time for the varying time step size $\Delta t = 0.2, 0.1, 0.05, 0.02, 0.01, 1/h^2$ with fixed mesh size $1/32$. Notably, the results demonstrate that the absence of SAV technical support prevents the algorithm from stabilizing at larger time step sizes.

Moreover, to better display that the proposed ensemble algorithms are unconditionally stable, we check the energy attenuation results of A1 and A2 as representatives under different time steps. As illustrated in Figs. 3(c)-3(d), we plot the evolution of $0.5 * \|u_1^{n+1}\|^2 + 0.5 * \|u_2^{n+1}\|^2$ in time for the varying time step size $\Delta t = 0.2, 0.1, 0.05, 0.02, 0.01$ with fixed mesh size $1/32$. We note that, for fixed h, with the different time steps Δt, the energy of A1 and A2 decreases rapidly with the increase of time and tends to be stable. More importantly, the smaller the time steps Δt, the quicker we reach the steady case. Generally, the observation shows that the time step conditions are not necessary, which can indicate that the proposed algorithms are unconditionally stable.

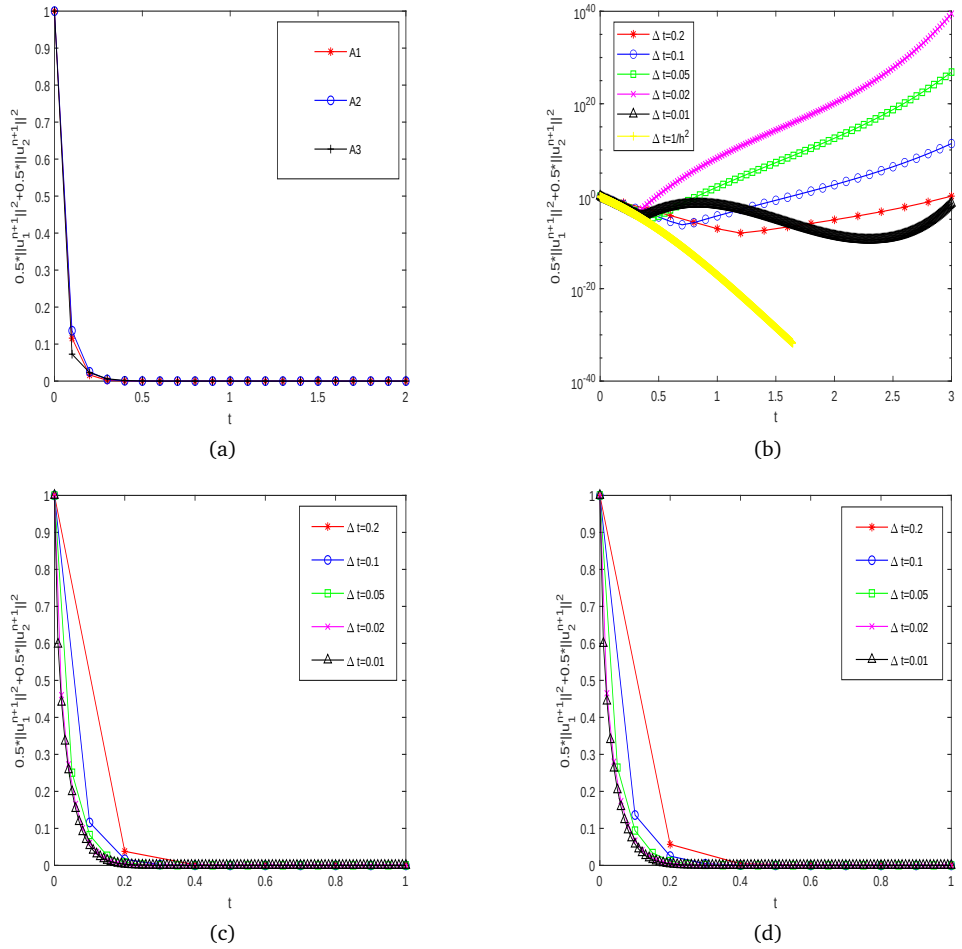

Figure 3: Energy versus time of three proposed ensemble algorithms on large time step points with $\Delta t = 0.1$ while $h = 1/32$ (a). (b) Show the evolution of $0.5 * \|u_i^{n+1}\|^2 + 0.5 * \|u_2^{n+1}\|^2$ in time for the varying time step size $\Delta t = 0.2, 0.1, 0.05, 0.02, 0.01, 1/h^2$ with fixed $h = 1/32$ for the A1 algorithm without SAV. The evolution of $0.5*\|u_i^{n+1}\|^2+0.5*\|u_2^{n+1}\|^2$ in time for the varying time step size $\Delta t = 0.2, 0.1, 0.05, 0.02, 0.01$ with fixed $h = 1/32$ for the A1 algorithm (c) and the A2 algorithm (d).

5.3. Random steel-titanium composite plate fuel cell model

Composite materials are widely used in life and production due to their environmental protection, low cost and excellent mechanical properties. Examples of such materials are steel-titanium composite plates, copper-aluminium composite plates, etc. These composite plates are the key components of the metal bipolar plate material for the fuel cell. The performance and lifespan of the cell are influenced by temperature, and the thermal management of the cell has attracted a lot of attention. Therefore, motivated by the above application, we design a random steel-titanium composite plate fuel cell model to investigate its internal heat conduction phenomenon.

We assume two materials can be expressed explicitly as $[0,2]\times[0,2]\times[0,4]\cup[2,4]\times[0.5,1]\times[2,3]\cup[6,8]\times[0,2]\times[2,4]\cup[4,6]\times[0.5,1]\times[2,3]$ in the conceptual domain, see Fig. 4. For simplicity, we only give the leftmost heat of the steel plate as Dirichlet boundary condition $u_1(t)=20$ and assume other surfaces of the whole model (excluding the interface) as homogeneous Neumann boundary conditions $\nabla u_i(t)\cdot\hat{n}_i=0$. The initial conditions are presumed to be 0 and there is no external force term. Owing to the random fiction parameter κ does not need a small perturbation constraint, we select ten samples for the random κ, which are $0.001, 0.005, 0.01, 0.05, 0.1, 0.5, 1, 5, 10, 50$. According to Wikipedia, the heat conductivity of steel is usually between 51.9 and 67.4 due to the different carbon content, and the heat conductivity of titanium is about $15.6-22.5$. Hence, in the above selection interval, we randomly selected ten samples for the Monte Carlo simulation.

We utilize the A1 and A2 algorithms with $h=1/16$ and $\Delta t=0.01$ to simulate the heat transfer process inside the steel-titanium composite plate fuel cell model, as depicted in Figs. 5 and 6, respectively. With the increase of time, the heat is gradually transferred from the steel plate to the titanium plate, and because the steel plate has

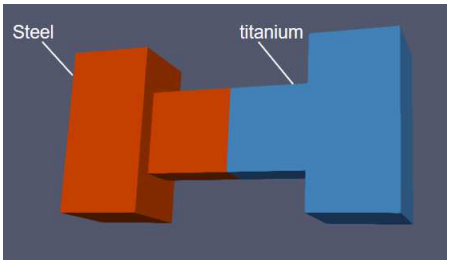

Figure 4: The conceptual domain of steel-titanium composite plate full cell model.

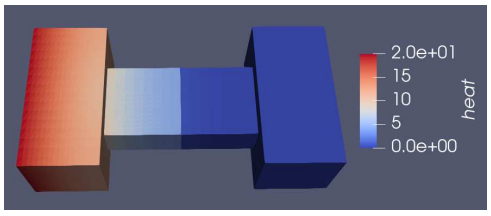

(a) $t=0.05$

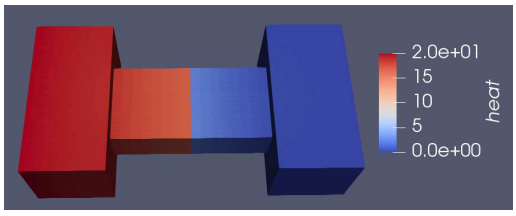

(b) $t=0.2$

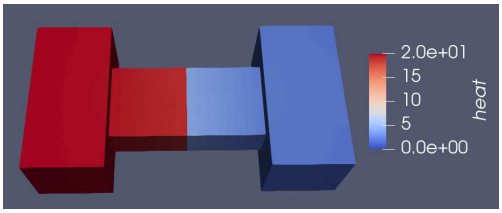

(c) $t=1.0$

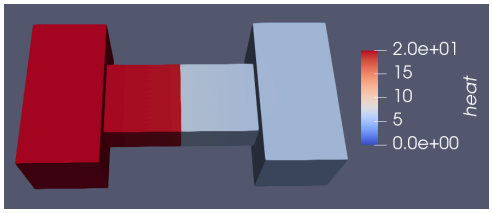

(d) $t=4.0$

Figure 5: Heat conduction in the random steel-titanium composite plate fuel cell model with $h=1/16$ and $\Delta t=0.01$ by A1 algorithm.

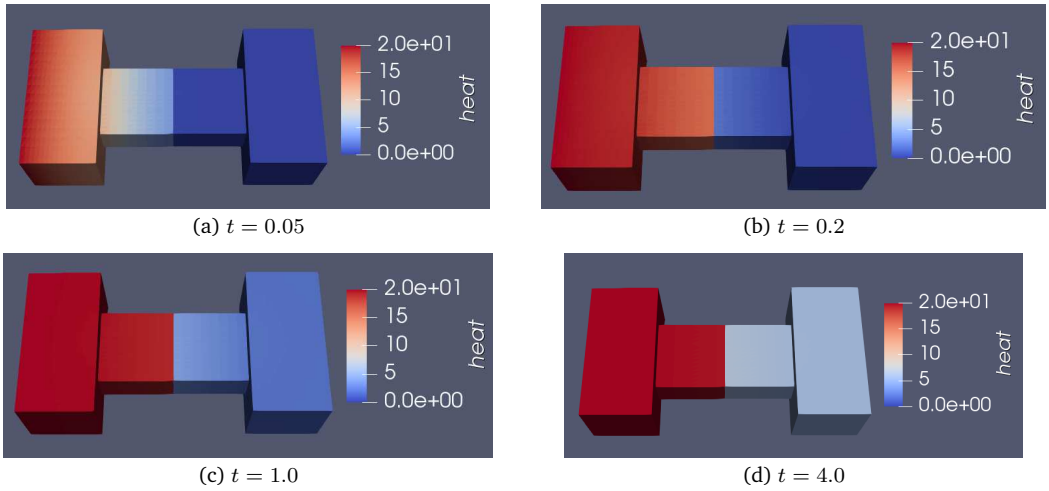

(a) $t = 0.05$ (b) $t = 0.2$

(c) $t = 1.0$ (d) $t = 4.0$

Figure 6: Heat conduction in the random steel-titanium composite plate fuel cell model with $h = 1/16$ and $\Delta t = 0.01$ by A2 algorithm.

a relatively high heat conductivity, it can be heated rapidly. Moreover, there is a significant jump at the interface between the steel plate and the titanium plate influenced by the friction parameter. In summary, all discussions further guarantee the effectiveness of our proposed algorithms.

6. Conclusion

We first introduce the Monte Carlo algorithm and demonstrate that its convergence is influenced by both the Monte Carlo method and classical numerical methods. Then, our primary focus is on proposing innovative numerical methods for the second step of the Monte Carlo algorithm. We establish an unconditional stable algorithm for the IMEX scheme by combining the ensemble idea and SAV method. Then, for the data-passing scheme, two ensemble algorithms without any auxiliary variables are established with the three random parameters κ, ν_1 and ν_2, which can also achieve unconditional stability. This kind of idea can also be extended to the nonlinear fluid-fluid problem.

References

[1] M. D. A. Al Mahbub, X. He, N. J. Nasu, C. Qiu, Y. Wang, and H. Zheng, *A coupled multiphysics model and a decoupled stabilized finite element method for the closed-loop geothermal system*, SIAM J. Sci. Comput. 42 (2020), 951–982.

[2] D. Bresch and J. Koko, *Operator-splitting and Lagrange multiplier domain decomposition methods for numerical simulation of two coupled Navier-Stokes fluids*, Int. J. AP. Mat. Com-Pol. 16 (2006), 419–429.

[3] Y. CAO, M. GUNZBURGER, X. HU, F. HUA, X. WANG, AND W. ZHAO, *Finite element approximations for Stokes-Darcy flow with Beavers-Joseph interface conditions*, SIAM J. Numer. Anal. 47 (2010), 4239–4256.
[4] Q. CHENG, C. LIU, AND J. SHEN, *Generalized SAV approaches for gradient systems,* J. Comput. Appl. Math. 394 (2021), p.113532.
[5] J. CONNORS, *An ensemble-based conventional turbulence model for fluid-fluid interaction*, Int. J. Numer. Anal. Mod. 5 (2018), 492–519.
[6] J. M. CONNORS, J. S. HOWELL, AND W. J. LAYTON, *Partitioned time-stepping for a parabolic two domain problem*, SIAM J. Numer. Anal. 47 (2009), 3526–3549.
[7] J. M. CONNORS, J. S. HOWELL, AND W. J. LAYTON, *Decoupled time stepping methods for fluid-fluid interaction*, SIAM J. Numer. Anal. 50 (2012), 1297–1319.
[8] D. HAN, X. WANG, AND H. WU, *Existence and uniqueness of global weak solutions to a Cahn-Hilliard-Stokes/Darcy system for two phase incompressible flows in karstic geometry*, J. Differential Equations 257 (2014), 3887–3933.
[9] F. HECHT, *New development in freefem++*, J. Numer. Math. 20 (2012), 251–265.
[10] Y. HOU AND D. XUE, *Numerical analysis of two-grid decoupling finite element scheme for Navier-Stokes/Darcy model*, Comput. Math. with Appl. 113 (2022), 45–51.
[11] F. HUANG, J. SHEN, AND Z. YANG, *A highly efficient and accurate new scalar auxiliary variable approach foe gradient flows,* SIAM J. Sci. Comput. 42 (2020), A2514–A2536.
[12] N. JIANG AND W. J. LAYTON, *An algorithm for fast calculation of flow ensemble,* Int. J. Uncertain. Quanti. 4 (2014), 273–301.
[13] N. JIANG AND W. J. LAYTON, *A higher order ensemble simulation algorithm for fluid flows,* J. Sci. Comput. 64 (2015), 264–288.
[14] N. JIANG AND W. J. LAYTON, *Numerical analysis of two ensemble eddy viscosity numerical regularizations of fluid motion,* Numer. Methods Partial Differ. Equ. 31 (2015), 630–651.
[15] N. JIANG AND W. J. LAYTON, *An efficient ensemble algorithm for numerical approximation of stochastic Stokes-Darcy equations,* Comput. Methods Appl. Mech. Engrg. 343 (2019), 249–275.
[16] W. J. LAYTON, F. SCHIEWECK, AND I. YOTOV, *Coupling fluid flow with porous media flow*, SIAM J. Numer. Anal. 40 (2003), 2195–2218.
[17] W. LI, P. HUANG, AND Y. HE, *An unconditionally stable finit element scheme for a nonlinear fluid-fluid interaction model,* Ima. J. Numer Aana. 00 (2023), 1–35.
[18] X. LI, J. SHEN, AND Z. LIU, *New SAV-pressure correction methods for the Navier-Stokes equations: Stability and error analysis,* Math. Comput. 91 (2022), 141–167.
[19] X. LI, W. WANG, AND J. SHEN, *Stability and error analysis of IMEX SAV schemes for the magneto-hydrodynamic equations,* SIAM J. Numer. Anal. 60 (2022), 1026–1054.
[20] J. L. LIONS, R. TEMAM, AND S. WAN, *Models for the coupled atmosphere and ocean (CAO I)*, Comput. Mech. Adv. 1 (1993), 1–54.
[21] J. L. LIONS, R. TEMAM, AND S. WAN, *Numerical analysis of the coupled atmosphere-ocean models (CAO II)*, Comput. Mech. Adv. 1 (1993), 55–119.
[22] J. L. LIONS, R. TEMAM, AND S. WAN, *Mathematical theory for the coupled atmosphere-ocean models (CAO III)*, Comput. Mech. Adv. 74 (1995), 105–163.
[23] Y. LUO AND Z. WANG, *An ensemble algorithm for numerical solutions to deterministic and random parabolic PDEs,* SIAM J. Numer. Anal. 56 (2018), 859–876.
[24] Y. LUO AND Z. WANG, *A multilevel Monte Carlo ensemble scheme for solving random parabolic PDEs*, SIAM J. Sci. Comput. 41 (2019), A622–A642.
[25] M. MOHEBUJJAMAN AND L. G. REBHOLZ, *An efficient algorithm for computation of MHD flow ensembles,* Comput. Methods Appl. Math. 17 (2017), 121–137.

[26] J. SHEN AND J. XU, *Convergence and error analysis for the scalar auxiliary variable (SAV) schemes to gradient flows,* SIAM J. Numer. Anal. 56 (2018), 2895–2912.
[27] J. SHEN, J. XU, AND J. YANG, *The scalar auxiliary variable (SAV) approach for gradient flows,* J. Comput. Phys. 353 (2018), 407-–416.
[28] Y. SUN, W. SUN, AND H. ZHENG, *Domain decomposition method for the fully-mixed Stokes-Darcy coupled problem*, Comput. Methods. Appl. Mech. Engrg. 374 (2021), p. 113578.
[29] Y. ZHANG, Y. HOU, AND L. SHAN, *Error estimates of a decoupled algorithm for a fluid-fluid interaction problem*, J. Comput. Appl. Math. 333 (2018), 266–291.